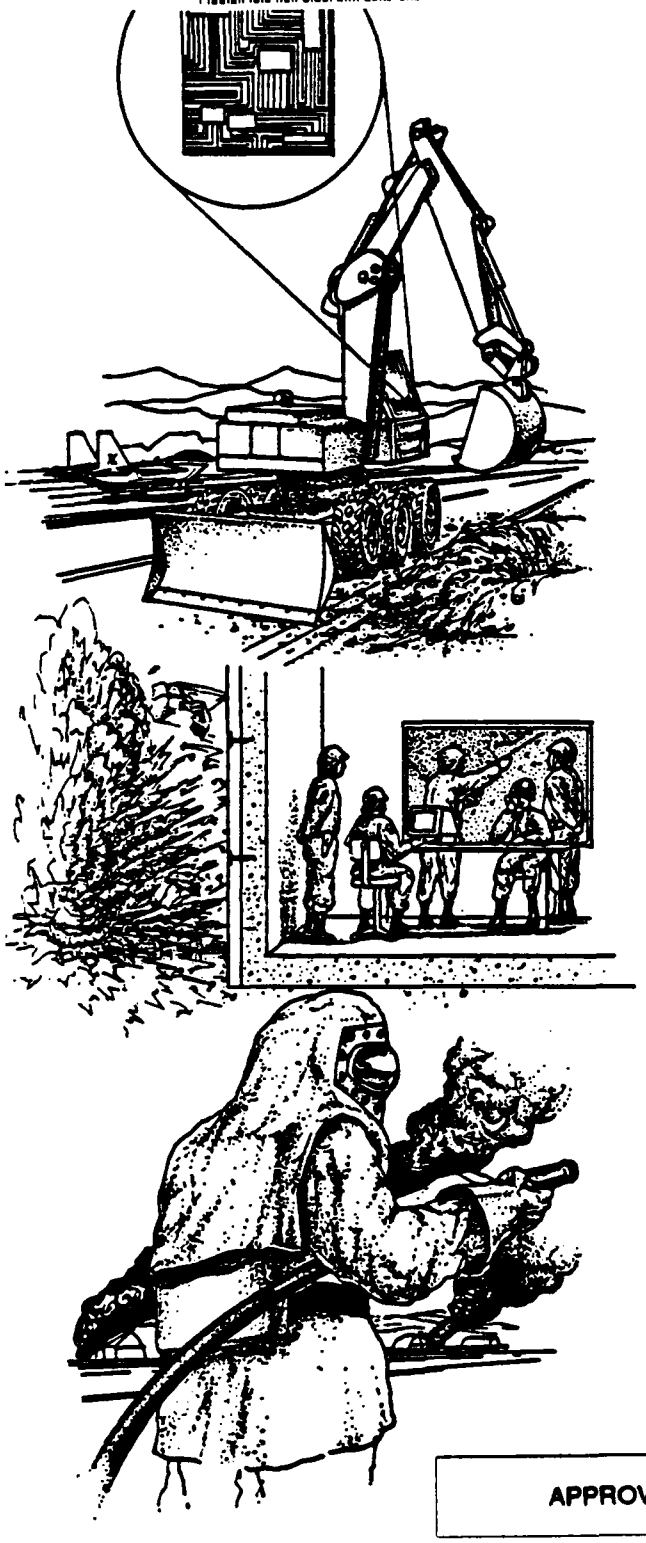
AD-A245 096



ESL-TR-89-50

INITIAL FIRE SUPPRESSION REACTIONS OF HALONS PHASE II-VERIFICATION OF EXPERIMENTAL APPROACH AND INITIAL STUDIES

E.A. WALTERS, J.S. NIMITZ, R.E. TAPSCOTT, G.D. BRABSON, J.H. MAY, J.T. CLAY, JR., D.L. ARNEBERG, M.H. WALL, H.D. BEESON AND T.A. MOORE

NEW MEXICO ENGINEERING RESEARCH INSTITUTE
UNIVERSITY OF NEW MEXICO
ALBUQUERQUE NM 87131

SEPTEMBER 1990

FINAL REPORT

JUNE 1988 — APRIL 1989

DTIC
ELECTE
JAN 27 1992
S B D

APPROVED FOR PUBLIC RELEASE: DISTRIBUTION UNLIMITED

ENGINEERING RESEARCH DIVISION
Air Force Engineering & Services Center
ENGINEERING & SERVICES LAB
Tyndall Air Force Base, Florida

92-01832

92 1 22 066

The following commercial product (requiring Trademark®) is mentioned in this report. Because of the frequency of usage, the Trademark was not indicated.

Unify

The following copyrighted product (requiring Copyright©) is mentioned in this report. Because of the frequency of usage, the Copyright was not indicated.

NMERI HALOCARBON DATABASE

If it becomes necessary to reproduce any segment of this document containing any of these names, this notice must be included as part of that reproduction. Mention of the products listed above does not constitute Air Force endorsement or rejection of this product, and use of information contained herein for advertising purposes without obtaining clearance according to existing contractual agreements is prohibited.

NOTICE

PLEASE DO NOT REQUEST COPIES OF THIS REPORT FROM
HQ AFESC/RD (ENGINEERING AND SERVICES LABORATORY).
ADDITIONAL COPIES MAY BE PURCHASED FROM:

NATIONAL TECHNICAL INFORMATION SERVICE
5285 PORT ROYAL ROAD
SPRINGFIELD, VIRGINIA 22161

FEDERAL GOVERNMENT AGENCIES AND THEIR CONTRACTORS
REGISTERED WITH DEFENSE TECHNICAL INFORMATION CENTER
SHOULD DIRECT REQUESTS FOR COPIES OF THIS REPORT TO:

DEFENSE TECHNICAL INFORMATION CENTER
CAMERON STATION
ALEXANDRIA, VIRGINIA 22314

REPORT DOCUMENTATION PAGE

Form Approved
OMB No. 0704-0188

Public reporting burden for this collection of information is estimated to average 1 hour per response, including the time for reviewing instructions, searching existing data sources, gathering and maintaining the data needed, and completing and reviewing the collection of information. Send comments regarding this burden estimate or any other aspect of this collection of information, including suggestions for reducing this burden, to Washington Headquarters Services, Directorate for information Operations and Reports, 1215 Jefferson Davis Highway, Suite 1204, Arlington, VA 22202-4302, and to the Office of Management and Budget, Paperwork Reduction Project (0704-0188), Washington, DC 20503.

1. AGENCY USE ONLY (Leave blank)	2. REPORT DATE	3. REPORT TYPE AND DATES COVERED
	September 1990	Technical Report June 1988 - April 1989

4. TITLE AND SUBTITLE
INITIAL FIRE SUPPRESSION REACTIONS OF HALONS PHASE II--VERIFICATION OF EXPERIMENTAL APPROACH AND INITIAL STUDIES

5. FUNDING NUMBERS
F29601-87-C-0001

6. AUTHOR(S)
Edward A. Walters, Jonathan S. Nimitz, Robert E. Tapscott, G. Dana Brabson, John H. May, James T. Clay, Jr., David L. Arneberg, Mark H. Wall, Harold D. Beeson, and Ted A. Moore

7. PERFORMING ORGANIZATION NAME(S) AND ADDRESS(ES)
New Mexico Engineering Research Institute
University of New Mexico
Albuquerque, New Mexico 87131

8. PERFORMING ORGANIZATION REPORT NUMBER
SS 2.08(2)

9. SPONSORING/MONITORING AGENCY NAME(S) AND ADDRESS(ES)
Engineering and Services Laboratory
Air Force Engineering and Services Center
Tyndall Air Force Base, Florida 32403

10. SPONSORING/MONITORING AGENCY REPORT NUMBER
ESL-TR-89-50

11. SUPPLEMENTARY NOTES
Availability of this report is specified on reverse of front cover.

12a. DISTRIBUTION/AVAILABILITY STATEMENT
Approved for public release;
distribution is unlimited.

12b. DISTRIBUTION CODE

13. ABSTRACT (Maximum 200 words)

This effort evaluated and verified experimental procedures for the characterization of the reactions and molecular products formed when halons enter flames. Initial studies using these procedures were also performed. Three techniques were studied to compare their usefulness for determining the concentrations of chemical species in flames: laser Raman spectroscopy, matrix isolation Fourier-transform infrared spectroscopy, and photoionization mass spectrometry. Laser Raman spectroscopy of hydrogen/oxygen flames extinguished with Halon 1301 provided identification of the principal flame species; however, this method was not effective in detecting minor species present in low concentration. The Raman spectrum of the hydrogen molecule was used to calculate flame temperatures. Matrix isolation experiments were used to characterize the fragmentation patterns of Halons 1211, 2402, and 1301. Of the three techniques, photoionization mass spectrometry was the most promising method for characterizing reactions occurring in flames. It was found that Halon 1211 does react with the free radical H, but the cross section of the overall process is small. No evidence was found for reactions between 0 atoms and either Halon 1211 or 1301. A database of fire suppression literature was developed and incorporated into the NMERI HALOCARBON DATA BASE.

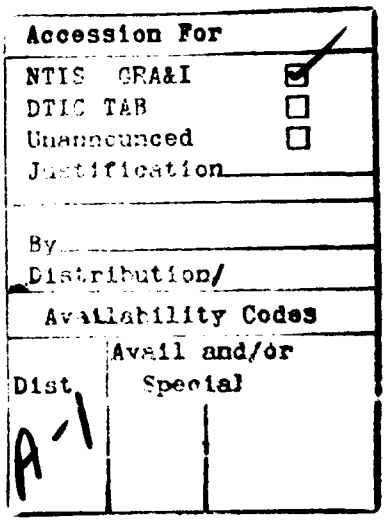
14. SUBJECT TERMS	15. NUMBER OF PAGES
Combustion, Halon, Raman, Spectroscopy, Matrix, Photoionization, Data base	
	16. PRICE CODE

17. SECURITY CLASSIFICATION OF REPORT	18. SECURITY CLASSIFICATION OF THIS PAGE	19. SECURITY CLASSIFICATION OF ABSTRACT	20. LIMITATION OF ABSTRACT
UNCLASSIFIED	Unclassified	Unclassified	Unclassified

EXECUTIVE SUMMARY

This effort evaluated and verified experimental procedures for the characterization of the reactions and molecular products formed when halons enter flames. It also included the performance of initial studies using those procedures. Three techniques were studied to compare their usefulness for determining the concentrations of chemical species in flames: laser Raman spectroscopy, matrix isolation Fourier-transform infrared spectroscopy, and photoionization mass spectrometry. Laser Raman spectroscopy of hydrogen/oxygen flames extinguished with Halon 1301 provided identification of the principal flame species; however, this method was not effective in detecting minor species present in low concentrations. The Raman spectrum of the hydrogen molecule was used to calculate flame temperatures. The purpose of the matrix isolation experiments was to characterize the fragmentation patterns of Halons 1211, 2402, and 1301. The expected fragments and some stable molecules were observed. Of the three techniques, photoionization mass spectrometry was found to be the most promising method for characterizing reactions occurring in flames. It was found that Halon 1211 does react with the free radical H, but the cross section of the overall process is small. No evidence was found for reactions between O atoms and either Halon 1211 or 1301. A database of fire suppression literature was developed and incorporated into the NMERI HALOCARBON DATABASE, and an experimental plan for Phase III was developed.





(The reverse of this page is blank.)

PREFACE

This report was prepared by the New Mexico Engineering Research Institute (NMERI), University of New Mexico, Albuquerque, New Mexico 87131. Portions of the work described here were sponsored by the Air Force Engineering and Services Laboratory, Air Force Engineering and Services Center, Tyndall Air Force Base, Florida, 32403, through contracts F29601-84-C-0080 and F29601-87-C-0001 under the Weapons Laboratory, Kirtland Air Force Base, Albuquerque.

This report summarizes work done between June 1988 and April 1989. The HQ AFESC/RDCF Project Officers were Major E. Thomas Morehouse and Capt John R. Floden.

Professors Thomas M. Niemczyk and Fritz S. Allen, of the University of New Mexico Department of Chemistry, provided comments, suggestions, and technical assistance on the laser Raman studies. Major E. Thomas Morehouse, Jr., Project Manager, and Mr. Joseph L. Walker, Chief, Fire Technology Branch, Air Force Engineering and Services Laboratory, provided information and discussions for successful completion of the project.

This report has been reviewed by the Public Affairs Officer (PA) and is releasable to the National Technical Information Service (NTIS). At NTIS it will be available to the general public, including foreign nationals.

This technical report has been reviewed and is approved for publication.

JOHN R. FLODEN, Capt, USAF
Project Officer

WILLIAM S. STRICKLAND
Chief, Engineering Research Division

JOSEPH L. WALKER
Chief, Air Base Fire Protection
& Crash Rescue Systems Branch

FRANK P. GALLAGHER III, Col, USAF
Director, Engineering and Services
Laboratory

(The reverse of this page is blank.)

TABLE OF CONTENTS

Section	Title	Page
I	INTRODUCTION	1
	A. OBJECTIVE	1
	B. BACKGROUND	1
	C. SCOPE	2
	D. TECHNICAL APPROACH	2
	1. Verification of Experimental Approach	2
	2. Initial Studies of Halon Reactions	3
	3. Development of Experimental Plans	3
	4. Technology Database	3
	5. Final Report for Phases I and II	4
II	REVIEW OF PHASE I	5
	A. SCOPE OF THE PERTINENT LITERATURE	5
	B. TEMPERATURE MEASUREMENT	5
	C. TECHNIQUES FOR CHARACTERIZING FLAME SPECIES	6
	D. NUMERICAL MODELING	8
	E. MECHANISMS OF EXTINGUISHMENT	8
	F. TIME-RESOLVED EXPERIMENTS	10
	G. ALTERNATE EXTINGUISHMENT MECHANISMS	11
III	VERIFICATION OF EXPERIMENTAL APPROACH	12
	A. LASER RAMAN SPECTROSCOPY	12
	1. Aligning the Laser Optics	12
	2. Aligning the Monochromator Optics	15
	3. Installing the Burner	16
	4. Flame Temperature Measurements	20
	5. Theory of Raman Temperature Measurement	21
	6. Temperature Measurement Using the Hydrogen Raman Spectrum	27
	7. Results of Uninhibited H_2/O_2 Flame	30
	8. Results of Halon 1301 Inhibited H_2/O_2 Flame	33
	9. Comparison of Normal and Inhibited Flames	35

TABLE OF CONTENTS
(CONCLUDED)

Section	Title	Page
	B. MATRIX ISOLATION SPECTROSCOPY	38
	1. Introduction	38
	2. Experimental	39
	3. Results	41
	C. PHOTOIONIZATION MASS SPECTROMETRY	45
	1. Purpose	45
	2. Experimental	45
	3. Results	46
IV	RECOMMENDATIONS AND CONCLUSIONS	49
	A. LASER RAMAN SPECTROSCOPY	49
	B. MATRIX ISOLATION SPECTROSCOPY	55
	C. PHOTOIONIZATION MASS SPECTROMETRY	55
V	EXPERIMENTAL PLAN FOR PHASE III	57
APPENDIX		
A	DATABASE OF FIRE SUPPRESSION INFORMATION ON HALOCARBONS	59
	I INTRODUCTION	60
	A. BACKGROUND	60
	B. APPROACH	61
	II DATABASE	63
	A. HALOCARBON DATABASE CONFIGURATION	63
	B. LITERATURE DATABASE	64
	C. DATABASE USE	64
REFERENCES		72

LIST OF FIGURES

Figure	Title	Page
1	Raman Spectrometer, Showing Laser Optics and Monochromator Optics	13
2	Optical Setup Used to Translate the Horizontal Image of the Laser Passing Through the Flame to the Vertical Axis	14
3	Diagram for the Lens Equation	17
4	Burner Assembly	18
5	Raman Spectra of Oxygen in Air, and in a Highly Oxidizing Flame	23
6	Raman Spectrum Showing the Rotational/Vibrational Bands Used to Measure the Temperature of Hydrogen	28
7	Concentration Profiles of Hydrogen, Oxygen, and Water, Plus the Temperature Profile for an Uninhibited Hydrogen/Oxygen Flame	31
8	Concentration Profiles of Hydrogen, Oxygen, Halon 1301, and C_2, as Well as the Temperature Profile for a Halon 1301 Inhibited Hydrogen/Oxygen Flame	34
9	Temperature Profile of the Halon 1301 Inhibited Hydrogen/Oxygen Flame Showing the Temperature of the Flame Higher in the Flame	36
10	Principal Components of the Electric Discharge Supported Flame System	40
11	Data from Passing a Mixture of Argon, Halon 1301, and Varying Amounts of Hydrogen Through an Electric Discharge	43
A-1	NMERI HALOCARBON DATABASE Structure Version 2.0	62
A-2	NMERI HALOCARBON DATABASE Login Prompt	65
A-3	Report or Maintenance Selection Menu	65
A-4	Maintenance Selection Menu	66
A-5	Typical Literature Information Fields Contained in the NMERI HALOCARBON DATABASE	67

LIST OF FIGURES
(CONCLUDED)

Figure	Title	Page
A-6	Example Inquiry of the Author Field of the NMERI HALOCARBON DATABASE	69
A-7	Result of the Inquiry Shown on Figure A-6	70

LIST OF TABLES

Table	Title	Page
1	ENERGY DIFFERENCES BETWEEN ADJACENT VIBRATIONAL LEVELS FOR SEVERAL DIATOMIC SPECIES	24
2	PHOTOLYSIS EXPERIMENTS OF HALONS 1211 AND 1301 WITH FREE RADICAL PRECURSORS	47

LIST OF SYMBOLS

A	Arrhenius (pre-exponential) factor
c	Speed of light
$\vec{E}$	Electric field vector incident on the molecule
ΔE	Energy difference between molecular or atomic states
f	Focal length
$g_{v,J}$	Statistical weighting factor for a rovibrational state
h	Planck's constant
g_{Ni}	Nuclear spin degeneracy of the rotational state
ΔH	Enthalpy change (heat of reaction)
I	Intensity
I_o	Sample irradiance
J	Rotational energy level quantum number
k	Rate constant
k_b	Boltzmann's constant
$N_{v,J}$	Population of the v,J rovibrational state
Q_R	Rotational partition function
S	Distance from focusing lens
T	Absolute temperature
V	Vibrational energy level quantum number
ν	Frequency
$\underset{\approx}{\alpha}$	Polarizability tensor of the molecule along its principal coordinates
ϵ_o	Permittivity of free space
$\Delta\nu$	Change in wavelength
ω_o	Frequency of incident light
ω_k	Frequency of vibration of the molecule along its k^{th} normal coordinate

(The reverse of this page is blank.)

SECTION I
INTRODUCTION

A. OBJECTIVE

The objective of this effort is to evaluate an experimental approach and initiate work to determine the initial chemical reactions occurring when halon firefighting agents extinguish flames.

B. BACKGROUND

Halon firefighting agents have been used for many years. Because of their combination of effectiveness, cleanliness, safety, and relatively low cost, there has been little incentive to develop new chemicals. Recently, however, calculations and limited experimental data indicate that halons, like chlorofluorocarbons, deplete stratospheric ozone and contribute to global warming. The United States Air Force has been investigating alternative agents to replace halon suppressants (References 1-5). Knowledge of the initial reactions occurring when halons and other halocarbons extinguish flames is needed as a basis for the continuation of this halon replacement research. Halon fire suppression agents extinguish fires by terminating free-radical chain reactions. Though the final chemical reactions are relatively well understood, the reactions that first occur when halocarbon extinguishants enter flame fronts are almost entirely unknown. It is these initial reactions, however, that largely determine halon performance variations, effects of halon physical state on suppression, and effects of fire parameters on halon action. Investigations are needed to characterize the initial reactions leading to flame suppression when halon and halon-like extinguishants enter flames.

The first work on initial reactions of halons was performed in Phase II of the project "Next-Generation Fire Extinguishing Agent" (Reference 2). At that point it became apparent that the effort was sufficiently promising to warrant an independent project. Accordingly, a separate effort was

initiated. Work in Phase I, under Contract F29601-84-C-0080, Subtask 3.36, established an experimental protocol to determine the initial chemical reactions occurring when halon fire extinguishing agents are introduced into flames (Reference 6). In Phase I, an approach was developed, an experimental plan was prepared, and the instrumentation and facility necessary to continue with Phase II of the project were established. The work is continued here in Phase II, under a separate contract (F29601-87-C-0001).

C. SCOPE

The scope of this task involves a verification of experimental procedures developed for the identification and characterization of the reactions and molecular products formed when halons enter flames. The effort also includes the performance of initial studies using those procedures. The application of the results of this project to the development of materials to replace halon agents will be demonstrated, and experimentation for continuation of studies of initial reactions will be planned and justified.

D. TECHNICAL APPROACH

The following tasks were performed for Phase II of this project:

1. Verification of Experimental Approach

Sufficient experimental studies were performed to evaluate the ability of the approaches developed in Phase I, under Contract F29601-84-C-0080, Subtask 3.36, to characterize the initial reactions occurring when halon agents enter flames. These approaches are laser Raman spectroscopy, matrix isolation Fourier-transform infrared spectroscopy, and photoionization mass spectrometry. The studies included identification of selected molecular species in flames of hydrogen plus oxygen into which were introduced halons. The concentrations of selected species were also

determined for this extinguishing system. These studies also included characterization of reactions of free radicals with halons.

2. Initial Studies of Halon Reactions

Sufficient studies were performed to elucidate the principal fragmentation products and to propose reaction pathways and molecular mechanisms for the initial reactions occurring in interaction of halons with hydrogen/oxygen flames. Phase IIA included in this effort accomplished the development of methods for generating free radicals using photolysis, chemical methods, or other techniques. Methods for producing or tracking free radical reactions with halon molecules were developed. Selected free radical abstraction reactions involving halon molecules, or other reactions that appear to be significant to the flame suppression process and warrant further study, were characterized.

3. Development of Experimental Plans

Experimental plans are presented for a detailed Phase III study to verify the proposed initial reaction pathways and mechanisms in the work performed. Possible extension of the studies to other halocarbon extinguishants and fuels is discussed. A complete rationale for the direction selected for the Phase III work is presented. This rationale demonstrates the relationship of the work to the development of halon replacement agents. The plan includes a description of equipment and instrumentation needed. The Phase III studies are planned to advance work in progress on halon replacement.

4. Technology Database

The information obtained in the technology review performed in Phase I was used to construct a database of literature on both combustion and fire suppression. The database will be applied to the development of suppression concepts derived from the results of this and future phases.

The database will be used to develop proposed methodologies for prediction of flame suppression by halon-like chemicals. This database is described in Appendix A.

5. Final Report for Phases I and II

This final report reviews the results obtained in Phase I, details the results obtained in Phase II, presents conclusions, relates these conclusions to the search for alternatives to halon agents, and presents the plan for the Phase III studies.

SECTION II
REVIEW OF PHASE I

A. SCOPE OF THE PERTINENT LITERATURE

Because of the significant level of experimental activity over the past four decades, the literature contains several hundred papers pertaining directly to the extinguishment of flames by halogenated agents. When one adds the papers that treat general combustion and flame characterization and diagnostic techniques, the total number of papers is immense. For this reason, it is important that new research efforts be thoroughly examined before initiation and that experimental details be assessed by a comprehensive technology review.

B. TEMPERATURE MEASUREMENT

Although temporally and spatially resolved measurement of the temperature in a flame is not a trivial task, several techniques have been well worked out. The earliest methods used thermocouples, which can be made quite small and can be coated to prevent catalytic and/or reactive effects. The results can be corrected for radiation losses. Laser-optical techniques, especially laser Raman and coherent anti-Stokes Raman spectroscopy (CARS), are nonintrusive. These technologies take advantage of the fact that for a molecule in equilibrium in the flame, the relative populations of the various energy levels are directly related to the temperature. A recent technique combines physical (intrusive) sensing with optical monitoring. In this technique, a very thin silicon carbide filament is placed in the flame and optical pyrometric methods are used to determine the radiant emission temperature at each location along the filament.

C. TECHNIQUES FOR CHARACTERIZING FLAME SPECIES

Nonintrusive optical techniques for characterizing flames actually predate intrusive methods. Thus, flame emission spectroscopy is a traditional method for characterizing species present in various flame zones. Early on, this method was complemented with optical absorption experiments.

Relatively recently, probes have been inserted into flames to remove chemical species from selected flame locations. Two quite different types of probes have been used. Microprobes, which are very long and thin, are well suited for removing stable molecules but not for sampling radicals or ions, which react on the walls of the probe before reaching the analytical instrument. Large probes, with diameters of up to 1 centimeter, can be used to sample both stable species and radicals. In these latter probes, the flame species are drawn through a small orifice into the evacuated interior of the probe, thus forming a molecular beam that does not impinge on the walls of the probe and within which the various species do not collide.

The diagnostic instrument of choice for the microprobe experiments is the gas chromatograph, since it is well suited for separating and detecting small, stable molecules. The mass spectrometer is the instrument of choice for the molecular beam probe experiments. This instrument combines the very high sensitivity needed to detect species in the relatively low density molecular beam with the ability to identify both stable molecules and transient species such as radicals.

Although the application of molecular beam mass spectrometry to the characterization of flames peaked in the 1970s, excellent work using this technique continues to the present. In recent years, attention has turned to laser spectroscopic techniques because of their nonintrusive nature and their potential for high spatial and temporal resolution. Caution is warranted, however. These techniques, powerful as they are, have not proven to be suitable for all tasks. It should be noted, for example, that

spectroscopic monitoring of oxygen and hydrogen atom concentrations is difficult at best. Since the atoms absorb in the vacuum ultraviolet region of the spectrum, atmospheric gases must be rigorously excluded from the optical path. Even with this precaution, it may not be possible to monitor these atoms because of the strong absorption of normal flame components (O_2, N_2, etc.) in the vacuum ultraviolet region of the spectrum. Clear exceptions are shock tube and some reduced pressure experiments in which the flame gases are controlled to assure optical transparency at the wavelengths where hydrogen and oxygen atoms absorb.

Of all the optical techniques, laser-induced fluorescence (LIF) is the most sensitive. This technique is well suited for atoms and such small molecules as OH. The prerequisite for any fluorescence experiment is the existence of a suitable absorption band, one which permits excitation of the fluorescing state in the molecule (or atom) of interest. To excite the two most important flame species, hydrogen and oxygen atoms, one must use either multiphoton excitation or traditional vacuum ultraviolet atomic resonance fluorescence techniques. The latter technique is particularly applicable to shock tube or molecular-beam studies, wherein air is routinely rigorously excluded from the optical path.

While fluorescence techniques are well suited to some atoms and small molecules, laser Raman techniques have been applied to a large number of molecules and even to some atoms. The general applicability of Raman techniques stems from the fact that the species of interest is excited to a virtual state; the existence of a real state to which the species can be excited by the available laser wavelength is not required. This fact also accounts for the most severe limitation of laser Raman techniques: they are not very sensitive. Of the two most common Raman techniques, CARS differs from the simpler spontaneous Raman spectroscopy in that the CARS signal is coherent and emitted in a single direction, a characteristic that gives CARS the potential for greater sensitivity. In addition, CARS can be applied to sooting flames, where other techniques are severely impaired. This quality is especially significant since the addition of a halon generally increases

the visible luminescence and soot-generating characteristics of a flame. CARS, however, is technically a very difficult experiment.

Since Raman techniques are significantly less sensitive than fluorescence techniques, the former are best for examination of major flame species, but are not well suited for trace species. Consequently, much of the important chemistry can only be inferred from Raman experiments, while fluorescence techniques, at least in principle, permit direct observation of all species involved in the most important elementary reactions.

D. NUMERICAL MODELING

The inherent limitations of the available observational tools are of less importance today than they were in the past because of the substantial advances in numerical modeling of flames. Present models can include not only all of the elementary chemical reactions known to be important but also the molecular and thermal transport processes for the flame species. As a result, it is possible to draw inferences from available experimental data with increasing confidence. Indeed, while one would still like to measure all of the species involved in elementary reactions, it may now be possible to gain sufficient insight from the measurement of a subset. In particular, one may ask whether it is adequate to couple a Raman technique (for the measurement of fuel, oxidizer, and extinguishant) with LIF (for the measurement of OH) and computer modeling (to fill in the missing information about hydrogen atom and oxygen atom concentrations, mechanisms, and so on).

E. MECHANISMS OF EXTINGUISHMENT

Both physical and chemical mechanisms are believed to contribute to the extinguishment of flames by halons; however, the relative importance of each mechanism is debatable. Moreover, even though it is possible to draw a correlation between extinguishment efficiency and such physical properties as heat capacity, the importance of a chemical mechanism (which also correlates with physical properties) cannot be discounted. An obvious

experiment, one that would shed light on the relative importance of the two mechanisms, would compare the extinguishment efficiency of a preheated halon sample with that of a room-temperature sample.

Substantial evidence supports the conclusion that the principal role of CF_3Br is to provide bromine atoms, which catalyze the recombination of hydrogen atoms. It has also been suggested that, under some conditions, CF_3Br reacts with the OH radical (Reference 7) as shown in Reaction [1], although the evidence is much less conclusive.*

$$OH + CF_3Br \rightarrow CF_3 + HOBr, \Delta H(est., 298\ K) = +60\ kJ \qquad [1]$$

Further exploration of the importance of this reaction should be pursued using flow tube, bulb, or beam experiments. Frozen argon matrix isolation experiments might be considered as well. For these experiments, one may consider the thoroughly explored reaction of hydrogen atoms with NO_2, shown in Reaction [2], as a source of OH radicals (Reference 8).

$$H + NO_2 \rightarrow OH + NO \qquad [2]$$

One could monitor the disappearance of OH in a bulb or flow-tube experiment or search for reaction products by matrix isolation.

Though hydrogen bromide is a principal product of this experimental system, hydrogen fluoride is only a minor product. Ultimately, however, hydrogen fluoride is generated in substantial amounts. This observation suggests that Reactions [1] and [2] are but a part of a much more complex dynamic process. Important reactions leading to the production of HBr

*For the convenience of the reader, reaction numbers are placed in brackets and equation numbers are placed in parentheses throughout this report.

include the bromine abstraction Reactions [3] and [4], although the direct involvement of the H_2 molecule cannot be entirely discounted.

$$CF_3Br + H \rightarrow CF_3 + HBr, \quad \Delta H(298\ K) = -76\ kJ \qquad [3]$$

$$H + Br_2 \rightarrow HBr + Br, \quad \Delta H(298\ K) = -143\ kJ \qquad [4]$$

Although the principal mechanism for chemical extinguishment appears to be the catalytic recombination of hydrogen atoms by bromine, this reaction may not be dominant at all stoichiometries. An alternate mechanism could be important in the less studied fuel-lean region, which characterizes the boundary between a "natural" fire and the environment. In this context, it is likely that a search for alternative mechanisms may prove of great value.

F. TIME-RESOLVED EXPERIMENTS

Flame experiments conducted to date have been steady-state, where the effect of introducing the extinguishing agent has been studied as a function of the amount of extinguishant added. Many of these experiments have been done very well, and it would be of little value to repeat them. On the other hand, in order to understand fully the role of the extinguishant, it is essential to resolve the elementary reactions physically and to learn their reaction rates and temperature dependence. By doing so, intelligent alternatives to the simple halons might be identified. Such experiments are not straightforward; nevertheless, worthwhile approaches may involve the use of molecular beams or flow systems. Both of these techniques are powerful though instrumentation- and manpower-intensive. In addition, both require considerable preparatory work before appropriate combinations of reagents and conditions can be established. This preparatory work could consist of a set of bulb experiments in which early-reaction products of reactive free radicals, such as H, OH, Br, Cl, and I, are allowed to combine with halons. These radicals may be prepared by discharge methods or by laser multiphoton dissociation of precursors. Analysis of the products by infrared (IR) spectroscopy, mass spectrometry (MS), or gas chromatography (GC) will allow

identification. Another technique particularly suited to free-radical studies is electron paramagnetic resonance (EPR). Coupled with a flow system, EPR can give quantitative estimates of radical concentrations.

G. ALTERNATE EXTINGUISHMENT MECHANISMS

To this point, the emphasis has been placed primarily on experiments that focus on the extinguishment mechanism in which the concentration of hydrogen atoms is sharply reduced. However, it would be wise to complement these experiments with a set of experiments that focus on the reduction of hydroxyl free radicals. Two factors commend this approach. First, it is known that the O/H/OH system is essentially in equilibrium in the flame. Thus, any agent that reduces hydroxyl concentration (or oxygen atom concentration) will also reduce the hydrogen atom concentration and thus extinguish the flame. Second, the primary mechanism for destruction of potential depleters of stratospheric ozone during their passage through the troposphere is reaction with hydroxyl radicals. Photolysis by wavelengths longer than 300 nm also plays an important role. Thus, any agent that reacts with the hydroxyl radical not only should be an effective fire suppressant but also could be prevented from reaching the stratosphere by reactions with hydroxyl radicals in the troposphere. Indeed, it is conceivable that an agent that reacts with hydroxyl radicals as its primary extinguishment mechanism may not be a threat to the ozone layer. While such a research program is admittedly of higher risk than programs that focus on modification of conventional halon suppressants, such a program could provide the ultimate solution to the problem of ozone depletion by halons.

Based on the results for Phase I, in Phase II a project of methodology development was pursued to compare the usefulness of Raman spectroscopic techniques, matrix isolation FT-IR, and photoionization mass spectrometry.

SECTION III

VERIFICATION OF EXPERIMENTAL APPROACH

A. LASER RAMAN SPECTROSCOPY

1. Aligning the Laser Optics

The basic design of the Raman spectrometer is presented in Figure 1. The Raman spectrometer can be separated into two optical parts: the laser optics and the sample-to-monochromator optics (Figure 2). These two optical components must be aligned such that the signal arriving at the detector gives the highest signal-to-noise (S/N) ratio possible. In order to do this, one of the optical paths must be aligned first, and the other must then be aligned to it. Of the two optical paths, the laser component was the most difficult to align; therefore, it was the first to be aligned.

The laser optics are made up of two first surface mirrors and two 50-mm lenses. The first step in aligning the laser optics involved positioning the argon ion laser so that the beam was horizontal to the optical table. Alignment was accomplished by measuring the height of the laser beam above the optical table at two, well-spaced positions. Once this was achieved, the mirror used to direct the laser toward the expected position of the flame was installed. In order to align this mirror such that the beam remained parallel to the optical table, the mirror was first set so that it reflected the laser beam directly back along the path of the incident beam. It was then rotated in the plane of the optical table, so that it directed the beam toward the expected position of the flame. The back mirror was then installed and aligned by positioning it so that the laser beam reflected back along the path of the incident beam.

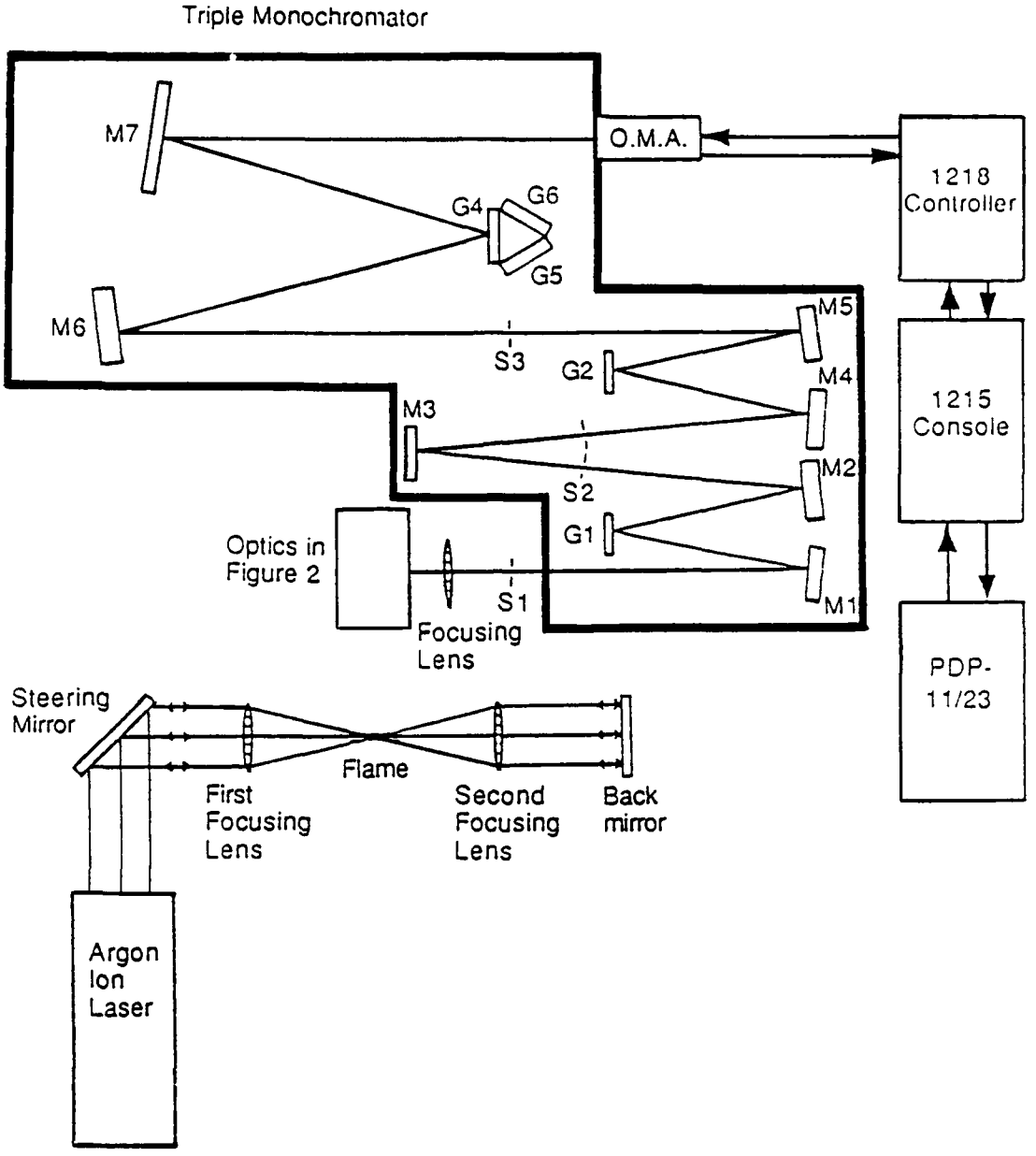


Figure 1. Raman Spectrometer, Showing Laser Optics and Monochromator Optics. Also shows electronic equipment required to acquire Raman spectrum. G stands for grating, M stands for mirror, S stands for slit.

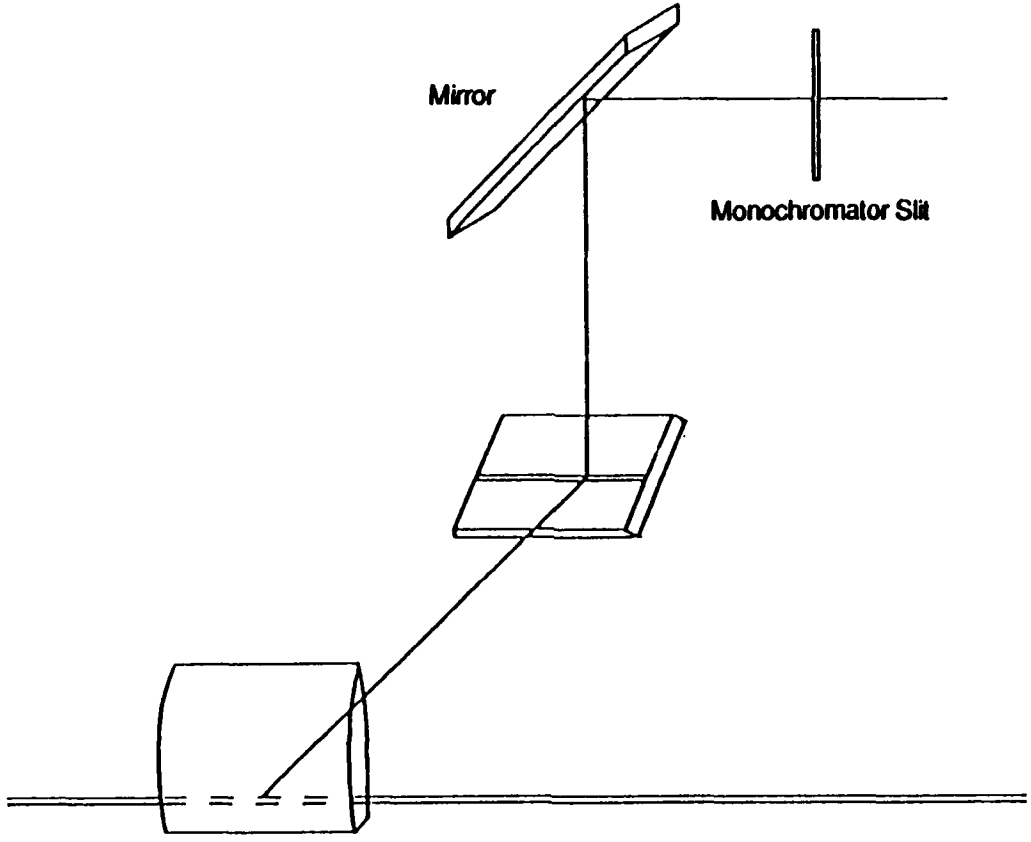


Figure 2. Optical Setup Used to Translate the Horizontal Image of the Laser Passing Through the Flame to the Vertical Axis.

At this point, the first lens could be installed. This lens could not be aligned as the mirrors were, since doing so caused the laser beam to diverge too much to allow one to determine adequately whether the reflected beam retraced the path of the incident beam. As a consequence, another method using the reflection of the laser off the outer and inner surfaces of the lens was employed. For this method, the lens was installed such that the reflection of the laser beam off the lens surfaces could be seen on the lab wall. If the lens was not aligned, two reflections could be seen. One reflection was caused by the beam entering the lens and the other by the beam exiting the lens. When the lens was aligned, a single spherical reflection, made up of the superposition of the two reflections from the lens, was seen.

The last step in aligning the laser optics was the installation of the second lens. This lens was placed between the first lens and the back mirror at approximately twice the focal point of the two lenses. Since this second lens was positioned so that it would, in conjunction with the first lens, collimate the laser beam, it could be aligned in much the same manner as the mirrors. The focal positions of the lenses were matched by observing the collimated beam returning to the laser cavity. When this beam appeared to be of the same diameter as the beam exiting the laser cavity, the focal points of the two lenses were considered matched, and the laser optics were considered aligned.

2. Aligning the Monochromator Optics

The next step involved in aligning the optics of the Raman spectrometer required aligning the sample-to-monochromator optics with the focal point between the two lenses in the laser optical path. In order to accomplish this, the optical multichannel analyzer (OMA) detector was replaced by a low-power alignment laser. When installed properly, the beam from the aligning laser followed the reverse path of the monochromator and exited from the center of the monochromator entrance slit. The beam was then used to align the mirror assembly, which was designed to translate the

Raman signal emanating from the horizontal argon ion laser beam to the vertical axis of the monochromator slits. The alignment was done by positioning the assembly such that the aligning laser beam exiting the monochromator intersected exactly the focal point between the two lenses focusing the argon ion laser beam. Finally, the 7.5-mm lens was placed between the mirror assembly and the focused argon ion laser beam according to the lens equation (1).

$$\frac{1}{S_1} + \frac{1}{S_2} = \frac{1}{f} \qquad (1)$$

where S_1, S_2, and f are the distances shown in Figure 3 (Reference 9). This lens was aligned by positioning it so that the alignment laser beam again intersected the argon ion beam at the focal point between the two lenses, thus focusing the argon ion beam.

Although the alignment of the optics for the Raman spectrometer may be complete, the above directions only allow the investigator to come close to exact alignment. The next and final step in aligning the optics requires that each element of both optical paths be individually adjusted to produce the maximum signal at the OMA detector. This time-consuming procedure may have to be repeated many times before the final alignment is achieved. Once the alignment is completed, however, there need be no more adjustments to either optical path unless one or more of the elements in either path is moved, by accident or necessity.

3. Installing the Burner

The burner is installed, as Figure 4 shows, with the slots running parallel to the argon ion laser beam (from here on called the "beam"). Furthermore, it is positioned so that the very center of the flame slot

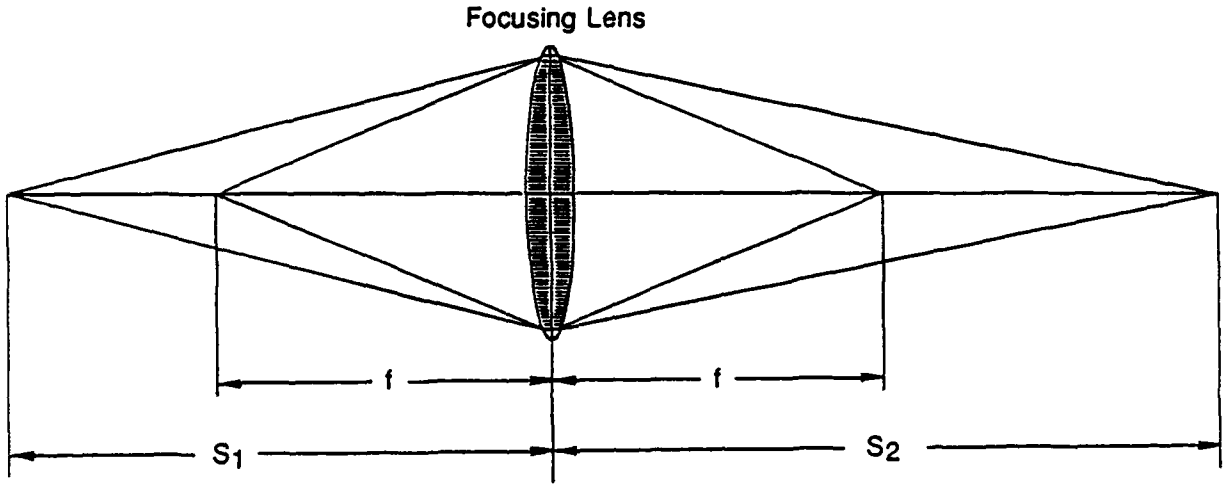


Figure 3. Diagram for the Lens Equation.

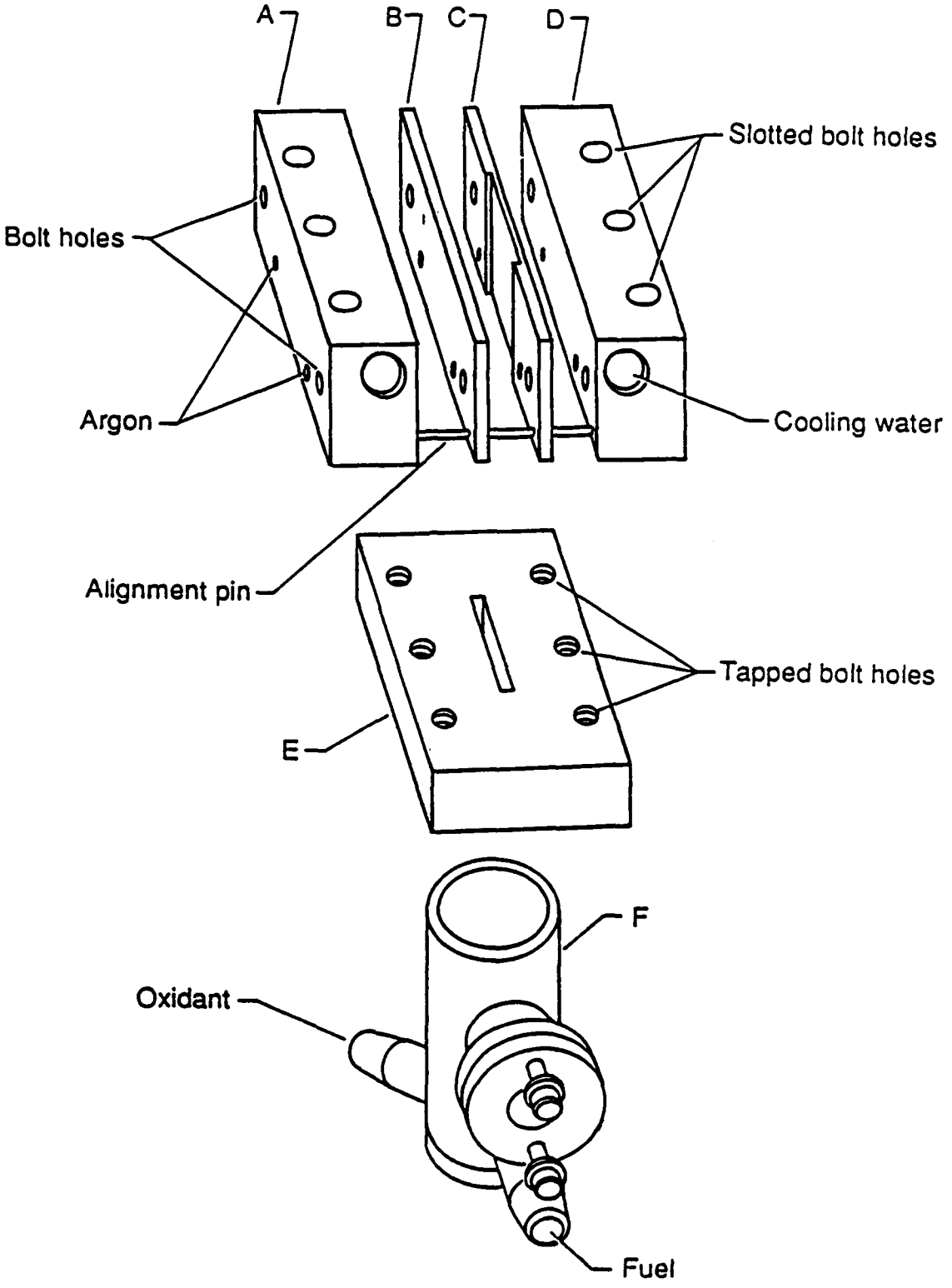


Figure 4. Burner Assembly. Parts A and D are 7.0 x 5.0 x 3.0 cm blocks with 0.04 indents machined into them. Part B is 7.0 x 0.3 x 3.0 cm spacer. Part C is a 7.0 x 0.34 x 3.0 cm spacer with a 0.4 cm indent. The dimensions of part E are 7.0 x 5.0 x 1.0 cm, and the slot in the center of the piece is 3.0 x 0.1 cm. Part F is a 5.0 cm high piece of 3.0 cm o.d., 2.0 cm i.d. tubing.

occurs at the focal point between the two lenses focusing the beam. Since the optics comprising the Raman spectrometer are fixed, the flame must be moved through the path of the laser beam. The burner was mounted on a platform that could be positioned by translational stages in either the x (parallel to the beam), y (horizontally perpendicular to the beam), or z (vertically perpendicular to the beam) directions. Once the x and y positions were set, data were recorded as a function of height above the burner by measuring the absolute position of the laser beam above the burner and then adding or subtracting the distance the z-translational stage had moved. The absolute height of the laser beam above the burner surface was measured by allowing the laser beam to burn a horizontal line in a piece of paper drawn across the burner surface. The distance between the position of the burn and the the bottom of the paper is equal to the height of the laser above the burner. Although this method seems crude, the burner height is reproducible. Accuracy, on the other hand, could easily be off by as much as 150 μm.

With the system aligned as described above, the cross section of the sample area (the cross section of the argon ion laser beam) focused on the monochromator entrance slit was measured to be a cylinder approximately 1 cm long, with a diameter of 250 μm. The slits on the monochromator were set at 300 μm for the main entrance slit and 200 μm for the entrance slit for the dispersion area of the monochromator. These slit widths were set by experimentally determining the combination that produced the best signal-to-noise (S/N) ratio for the system.

The procedure for acquiring data from the flame was as follows. Hydrogen gas was allowed to flow through the burner slot and was ignited by a spark. The oxygen gas was then turned on, and gas flows for both oxygen and hydrogen were set to values previously determined to provide a stable flame with a reaction zone approximately 2.5 mm above the burner surface for the uninhibited flame. The flame was allowed to burn for several minutes so that the system would come to equilibrium. The hydrogen flow rate was 16.25 liters per minute, the oxygen flow rate was 4.20 liters

per minute, the argon flow rate was 10.1 liters per minute, and the CF_3Br flow rate was 0.5 liters per minute. These rates were measured using the flow meter calibration curves provided by the Matheson Gas Company for each rotameter.

The monochromator was set to the region of the Raman spectrum desired. Data were gathered by first positioning the laser beam at a height 0.5 mm above the burner surface. The OMA was then set to acquire a Raman spectrum every eight seconds, for approximately 7 minutes. The 54 foreground scans, containing the Raman signal scattered from the flame, were combined and stored by the 1218 OMA console. Next, the laser was blocked, and a background spectrum was gathered exactly as the previous Raman spectrum. These two spectra, foreground and background, were then subtracted to produce the final Raman spectrum seen throughout this work. The burner was then moved down by 127 μm (0.005 inches), and the next spectral set was taken and stored. Data collection continued until the laser had passed through the combustion zone of the flame. The final height of the laser beam above the burner surface was measured to be 3.302 mm (0.130 inches). The 20 spectra taken at each region of the Raman spectrum investigated represented a pseudo-concentration profile of the molecules represented by the Raman bands. The minimum time required to obtain a full profile in any region of the Raman spectrum was 4 hours and 40 minutes. The actual time needed to acquire all the data for such a profile was more often 6 to 7 hours. This lengthy downtime was often due to warmup time and data acquisition problems that shut down the OMA detector during a scan.

4. Flame Temperature Measurements

The measurement of flame temperature is not a trivial task. A temperature probe would perturb the region of the flame where it is inserted, causing changes in the combustion process. As a consequence, the local temperature would also be changed. Recently, thermocouple devices capable of surviving the high temperatures of flames have been developed. These devices are designed to minimize flame perturbation; however, they

still produce erroneous results. Nonintrusive spectroscopic methods like sodium D line reversal (Reference 10), OH emission (References 11 and 12), Rayleigh (References 13 and 14), Raman (References 15-18), and fluorescence (Reference 10) have been used in the past. With the exception of Rayleigh scattering, these spectroscopic methods measure the populations of two or more of the electronic, vibrational, or rotational energy levels of a molecule. Knowing the populations of two or more energy levels of a molecule and their relative energies and degeneracies, one can calculate the temperature of that molecule using the Boltzmann equation.

Although spectroscopic measurements are less intrusive than thermocouple devices, they can still suffer such problems as a nonequilibrium population distribution, difficult spectroscopic setup, or inaccurate or imprecisely known transition probabilities (Reference 6). Consequently, no method is expected to produce the correct flame temperature without some modification of the equations used to calculate the temperature. Evidence of these problems can be found in the literature, where different methods have produced final flame temperatures that vary by 10 K or more (Reference 6).

The Raman spectrum of the hydrogen molecule was used to calculate the flame temperatures because this technique is the investigative tool for this work, and the temperature could be measured without changing the instrumental setup. The Raman method, used in conjunction with concentration data to evaluate the flame, was selected because the Raman temperature data were taken at the same time as the concentration data and, therefore, had the same spatial resolution.

5. Theory of Raman Temperature Measurement

The Raman spectrum of a molecule provides a large amount of information. Of particular interest is the effect of temperature on the spectrum of a molecule. If this effect can be measured, the temperature of the molecules in a flame can be calculated from the Raman spectrum. Two

Raman methods have been developed to measure flame temperatures. These are the Stokes/anti-Stokes method and the Stokes method (Reference 6). Both methods provide similar information, but the Stokes/anti-Stokes method requires considerably more difficult spectroscopic techniques than does the Stokes method. Thus, the Stokes method is the one of choice when determining the temperature of a flame using Raman spectroscopy.

Since the Raman spectrum of a molecule represents the population distribution among the vibrational and/or rotational states, molecular transitions between these states are used to determine the flame temperature. In the harmonic oscillator-rigid rotor model, the Raman spectrum of a ground-state molecule is identical to that of any excited state of that molecule. Fortunately, molecular vibrations and rotations are not perfect oscillators or rotators; therefore, the Raman spectra of the ground and excited states of a molecule are not identical (Reference 19). Consequently, the relative populations of the ground and excited states can be determined provided the shifts of the vibration or rotation frequencies are large enough to allow the Raman instrument to resolve the spectral bands. Normally, the anharmonicity within a normal vibration band causes a shift of only a few wavenumbers in the rotational components of the Raman spectrum. When the spectral shifts are this small, optical resolution of the different transitions is difficult. Because of the optical resolution of the instrument used in this work (4 to 8 cm^{-1}) and the effective broadening due to rotational/vibrational mixing, an energy difference of greater than 20 cm^{-1} is needed to resolve the Raman rotational transitions needed for temperature determinations (Figure 5).

Conveniently, some molecules, such as those in Table 1, have wavenumber shifts of up to several hundred wavenumbers. In particular, molecules such as the last three in Table 1, which have shifts of greater than 100 cm^{-1} for the ground and excited states, are reasonable candidates for measuring flame temperatures using Stokes Raman spectroscopy.

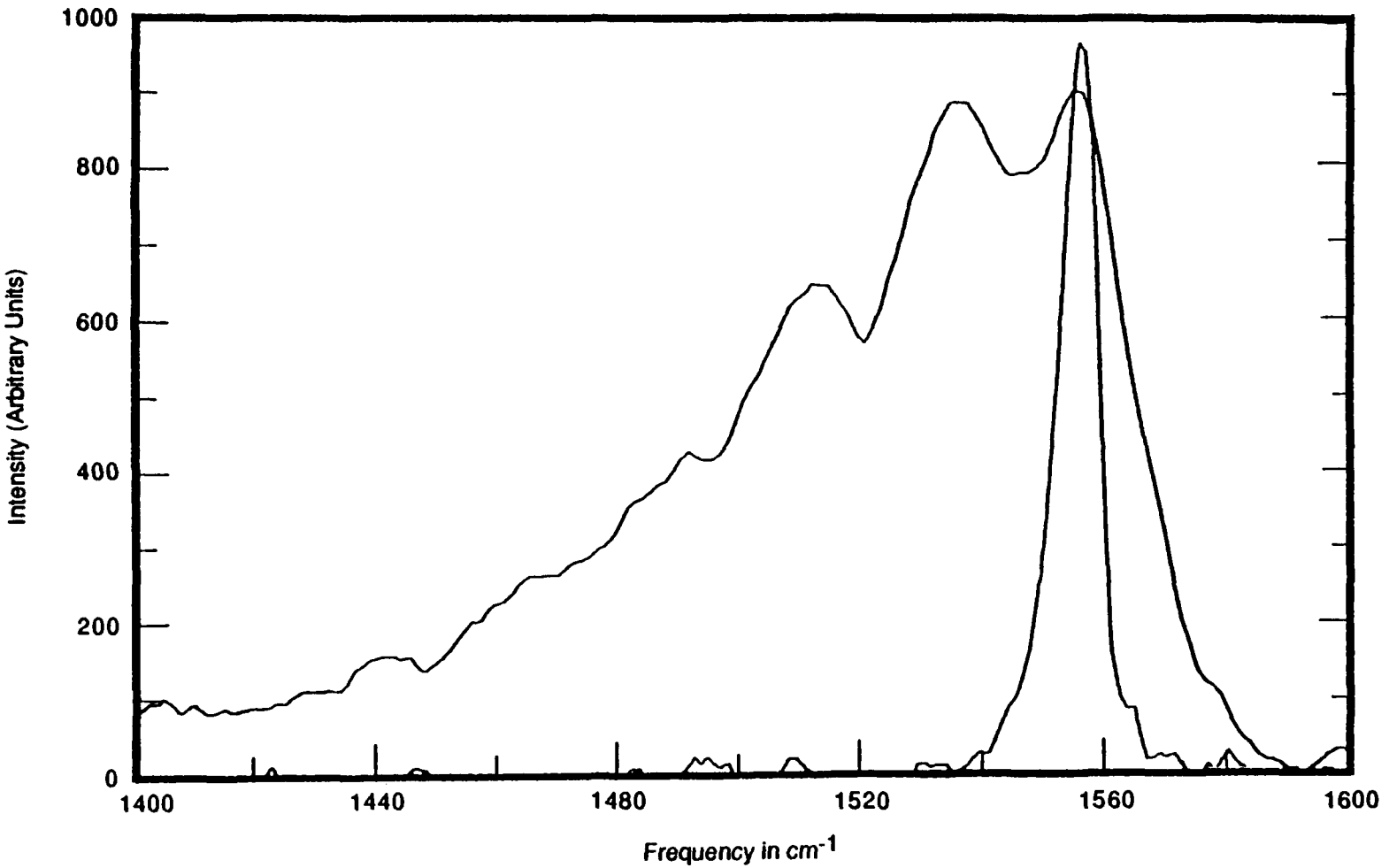


Figure 5. Raman Spectra of Oxygen in the Air, and in a Highly Oxidizing Flame. The narrow single band spectrum represents a room temperature spectrum of oxygen, while the broad multiband spectrum shows the excited states of the oxygen molecule due to increased temperature of the molecule. Temperature of the flame was not measured.

TABLE 1. ENERGY DIFFERENCES BETWEEN ADJACENT VIBRATIONAL LEVELS FOR SEVERAL DIATOMIC SPECIES.[a]

Molecule	Vibrational levels, $\Delta\nu(v + 1, v)$, cm^{-1}		
	1 → 0	2 → 1	3 → 2
O_2	23.7	23.3	23.0
N_2	28.8	28.8	28.8
HCl	103.6	103.3	102.9
OH	165.0	165.0	165.0
H_2	233.4	231.6	229.6

[a]Taken from Reference 15.

For the five molecules listed in Table 1, Raman spectroscopy gives lines spaced widely enough to permit accurate measurement of the intensities of the discrete rovibrational transitions. A relationship between the temperature and these spectra needs to be formulated so that flame temperatures can be measured. The expression for relating the spectral intensity to temperature is the Boltzmann equation (2) (Reference 20).

$$N_{v,J}/N = (g_{v,J}/Q_R) \exp(-\Delta E/k_b T) \qquad (2)$$

the molecule along its k^{th} normal coordinate, is called Stokes Raman scattering and is the effect with which this work is concerned.

Consider two transitions within the same band, for example, v" = 0, J" = 1 → v' = 1, J' = 1 and v" = 0, J" = 3 → v' = 1, J' = 3. Label the intensities of the lines I_{11} and I_{33}, respectively. Combining Equations (2) and (3), we obtain

$$I_{33}/I_{11} = N_{33}/N_{11} = g_{N3"}\ g_{3"}/g_{N1"}\ g_{1"}\ \exp\ [-(E_{3"}-E_{1"}/kT)] \qquad (4)$$

where g_{Ni} is the nuclear spin degeneracy of the rotational state, and the double primes are standard spectroscopic notation indicating the lower state. A measurement of the relative intensities of these lines permits calculation of the rotational temperatures in the flame.

$$I_{v+1} / I_v = (g_{v+1}/g_v)\exp\ (-\Delta E/kT) \qquad (5)$$

The rovibrational Raman spectrum of molecular hydrogen was chosen to measure the flame temperature for the following reasons:

a. Hydrogen is in high concentration in the precombustion zone (over 50 percent of the total gas is H_2).

b. The rovibrational Raman spectrum occurs in the region of 4156 cm^{-1}, well above most other molecules, so that little or no spectral interference is present.

c. The rovibrational Raman spectrum of hydrogen is an intense series of well-resolved Raman bands representing the Q branch of the fundamental hydrogen vibration, which allows easy access to the populations of two or more of the hydrogen rotational ground states.

It is important to note that rotational relaxation times are several orders of magnitude smaller than vibrational times (Reference 20).

where $N_{v,J}$ is the population of the v,J rovibrational state, $g_{v,j}$ is the statistical weighting factor, ΔE is difference in the energy between the v,J=0 and v,J rovibrational states, k_b is the Boltzmann constant, T is temperature, and Q_R is the rotational partition function. This equation relates the population of different rovibrational states of a molecule to the energy difference between those states and the temperature of the molecule. Therefore, the rotationally resolved Raman spectrum of a vibrational mode provides the energy difference between the rovibrational states and permits calculation of the population of each state. The energy difference is calculated directly from the wavenumber position of the Raman peak by the equation $E = hc\nu$, where h is Planck's constant, c is the speed of light, and ν is the frequency. Equation (3) indicates that the population of the ground rovibrational state v,J is proportional to the intensity of the Raman band, which arises from the transition from the vibrational state v,J to state v+1,J(ΔJ=0). For a sample of randomly oriented molecules the scattered radiant intensity, I, is given by

$$I = \frac{N_{v,J} I_o (\omega_o \pm \omega_k)^4 \underset{\approx}{\alpha}^2 E^2}{1440\, \pi^2 \epsilon_o^2} \qquad (3)$$

where ω_o is the frequency of the incident light, ω_k is the frequency of the vibration of the molecule along its k^{th} normal coordinate, $\underset{\approx}{\alpha}$ is the polarizability tensor of the molecule along its principal coordinates, $\vec{E}$ is the electric field vector incident on the molecule, ϵ_o is the permittivity of free space for an electric field, and I_o is the sample irradiance. The case of $\omega_o + \omega_k$, in which the frequency is higher than the incident frequency by an amount equal to the frequency of the vibrations of the molecule along its k^{th} normal coordinate, is called anti-Stokes Raman scattering.

The case of $\omega_o - \omega_k$, for which the frequency is lower than the incident frequency by an amount equal to the frequency of the vibrations of

Consequently, the population distribution for rotational states may more nearly reflect the equilibrium distributions than does the vibrational population distribution for a given flame temperature. Therefore, analysis of the Q branch of the hydrogen fundamental vibration may be expected to give temperatures closer to the true flame temperature than those obtained from rotationally unresolved vibrational spectra. This fact, along with the high signal intensity and low spectral interference of the hydrogen rovibrational spectrum, makes hydrogen the molecule of choice for the measurement of flame temperatures using Stokes Raman spectroscopy.

6. Temperature Measurement using the Hydrogen Raman Spectrum

The rovibrational Raman spectrum of hydrogen at room temperature can be seen in Figure 6. Superimposed on the experimental spectrum are vertical bars having locations calculated from the spectroscopic constants for H_2 and having amplitudes calculated from Equation (5), including the nuclear spin state degeneracies discussed below. One striking feature of the spectrum is the irregular band intensities, which are in contrast to the smooth transition from one band intensity to the next that might be expected. These irregular band intensities are due to statistical factors for homonuclear molecules like hydrogen. In the case of homonuclear diatomic molecules, the angular momenta of the two nuclei interact to produce a resultant angular momentum for the molecule and cause the statistical weight of the antisymmetrical level J to be less than the mean of the statistical weights of the neighboring symmetrical levels J+1 and J-1. For the hydrogen molecule a statistical weight ratio of 3:1 is expected for the symmetric and antisymmetric levels. Since the even rotational J levels of hydrogen are antisymmetric and the odd are symmetric, the Raman bands representing the transition originating from the odd rotational levels have a statistical weight of $3(2J + 1)$, while those from the even rotational levels have a statistical weight of only $(2J + 1)$. Therefore, an alternating intensity spectrum of the rovibrational Stokes Raman spectrum of H_2 is expected. When multiplied by the Boltzmann population factor, the intensities in Figure 6 result.

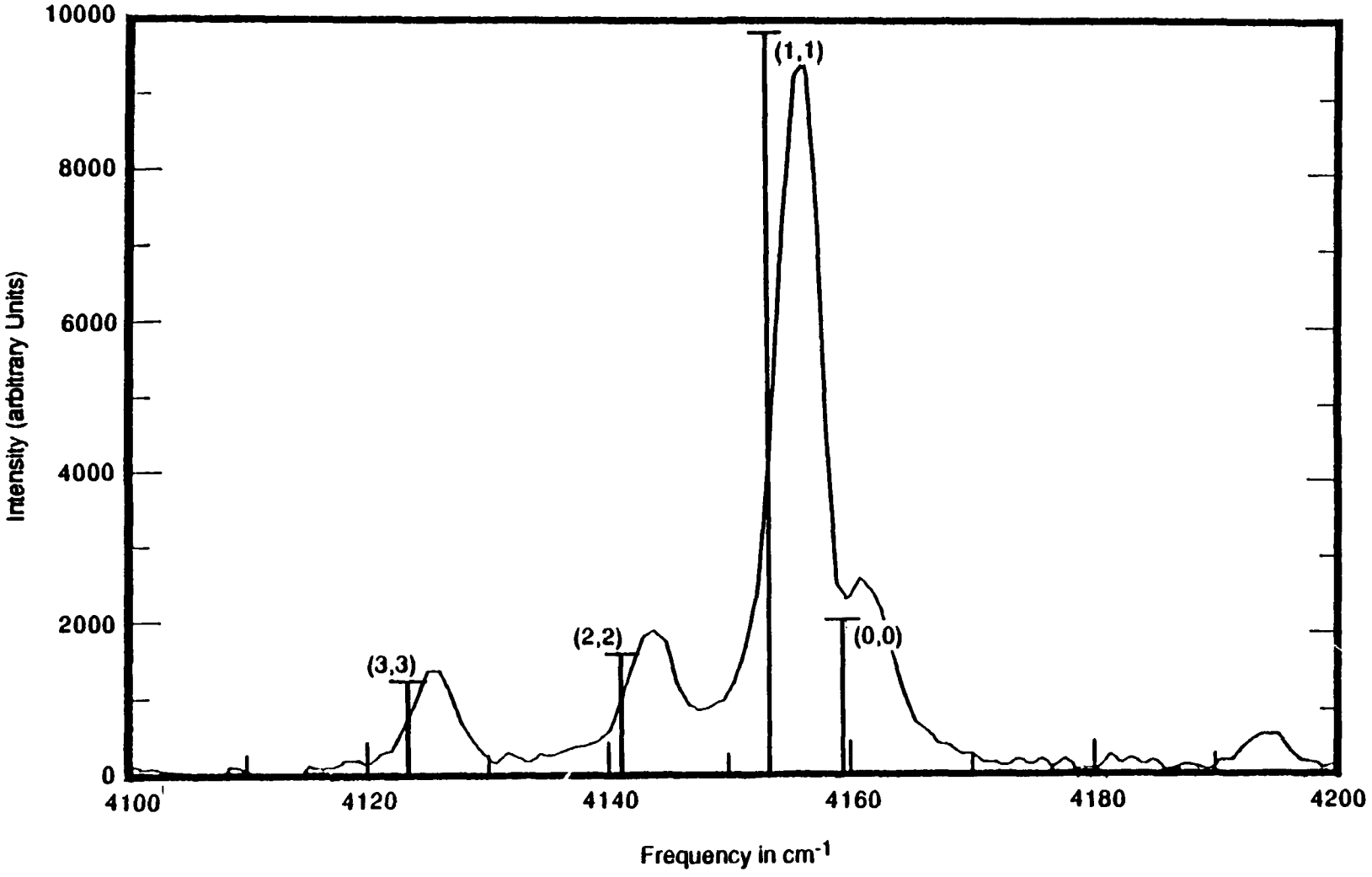


Figure 6. Raman Spectrum Showing the Rotational/Vibrational Bands Used to Measure the Temperature of Hydrogen. The most intense band is the Q(1,1) band, while the lowest energy band is the Q(3,3) band. The temperature of the hydrogen represented by this spectrum is 298.5 K.

In determining the temperature of the flame using the Q branch ($\Delta J = 0$) of the Raman Stokes hydrogen rovibrational spectrum, the intensities of the Raman bands for the 1",1' and the 3",3' rovibrational transitions were measured. These intensities are proportional to the fractional populations of the first and third rotational energy levels of the ground vibrational energy level. These two Raman bands were chosen because they are the most intense. This high intensity is due, in part, to the substantial state populations over the temperature range of interest and to the statistical weight of 3 to 1 for odd to even rotational energy levels in the H_2 rovibrational spectrum. Because the two bands chosen to measure the flame temperature are both odd, they have the same statistical weight due to the nuclear spin interactions. Consequently, the nuclear degeneracies cancel out and the statistical weights for the first and third rotational energy levels are simply 2J +1, where J is the rotational quantum number. The energy difference between the first and third rotational energy levels can be calculated from the pure rotational Raman spectrum of H_2 (Figure 5), where the $1 \rightarrow 3$ rotational transition (Reference 21) occurs at 587.027 cm^{-1} (1.166×10^{-20} Joules). Substitution into Equation (5) gives

$$\begin{aligned} N_{33}/N_{11} &= I_{33}/I_{11} \\ &= [2(3) + 1]/[2(1) + 1)]\exp(-1.166 \times 10^{-20}\text{Joules/kT}) \\ &= 7/3 \exp(-1.166 \times 10^{-20}\text{Joules/kT}) \end{aligned} \quad (6)$$

Solving Equation (6) for the temperature of the H_2 molecule and, therefore, the flame yields

$$T = (-1.166 + 10^{-20})/[k \ln (7I_1/3I_3)] \quad (7)$$

As an example of this technique, the intensities of the 1",1' and the 3",3' transitions, for the room temperature spectrum of hydrogen gas in Figure 4 were measured and found to be 3013 and 431 counts. Using Equation (7), the

calculated temperature is 302.5 K, which is very nearly that of the direct thermocouple measurement of 298.5 K.

In conclusion, the Raman method was chosen to measure the temperature of the flame for this work. Although the OH emission method is a well-established technique, it suffers from spatial resolution problems that severely reduce its usefulness here. The Raman method, having the same spatial resolution as the concentration measurements of the molecules in the flame, suffers from a decreased S/N ratio as the measurement approaches the reaction zone of the flame. This loss of S/N was not as important as the loss of spatial resolution of OH measurement because the present work is concerned with the precombustion zone of the flame where the lower S/N of the H_2 rovibrational spectrum can be tolerated.

7. Results of Uninhibited H_2/O_2 Flame

Three regions of the Raman spectrum were investigated for the uninhibited H_2/O_2 flame: the oxygen vibrational region at 1556 cm^{-1}, the water vibrational region at 3652 cm^{-1}, and the hydrogen rovibrational region at approximately 4156 cm^{-1}. The profiles obtained for each of these molecules in the uninhibited flame as well as the flame temperature are presented in Figure 7.

The important features of the concentration and temperature profiles presented in Figure 7 are the following:

a. The flat region in the hydrogen and oxygen profile, extending from 0.5 mm to approximately 1.25 mm, along with the low temperatures and low concentration of water in this region, indicates that this region is in the precombustion zone of the flame.

b. The rapid decrease in the concentrations of both hydrogen and oxygen beginning at approximately 1.25 mm above the burner and the increase

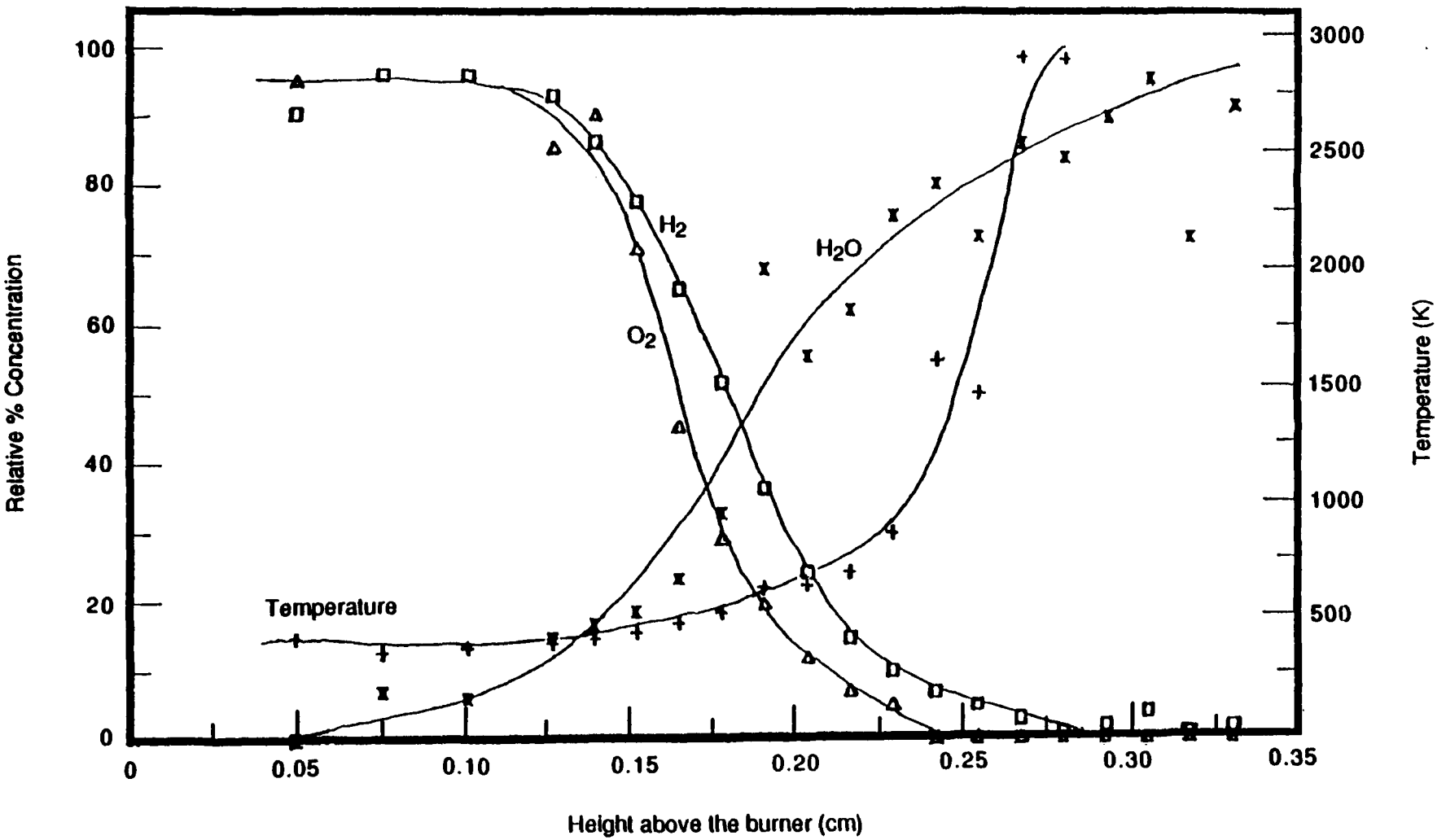


Figure 7. Concentration Profiles of Hydrogen, Oxygen, and Water, plus the Temperature Profile for an Uninhibited Hydrogen/Oxygen Flame. The gas mixture before combustion is 4:1 in H_2:O_2.

in the temperature of the flame after this point indicate the onset of the combustion zone.

c. The rapid rise in the temperature of the flame to a maximum of 3000 K in the region extending from 1.85 mm to 2.70 mm and the near depletion of both oxygen and hydrogen during this time indicate that this is the combustion zone of the flame.

d. Although the region higher than 2.70 mm above the burner is shown later in Figure 10, the high temperature and low and rapidly decreasing concentrations of the H_2 molecules in this region make temperature calculations unreliable.

Since this work is concerned with the reactions taking place in a halon-inhibited flame just prior to the combustion zone, the flame profiles shown in Figure 7 probe the region of the flame important to this study. Also, since the combustion zone of the Halon 1301-inhibited flame is expected to occur slightly farther from the burner surface than the normal flame, the extension of the normal flame profiles well into the combustion zone is necessary for direct comparison of the flame profiles of the two flames.

An interesting observation of the flame profile presented in Figure 7 is the complete destruction of the hydrogen molecule, despite the fact that the stoichiometry of the flame was approximately 4:1, hydrogen to oxygen. In order to understand this result, some properties of combustion and molecular transport must be reviewed. First, the H_2/O_2 reaction has a stoichiometry of $2H_2$ per O_2; therefore, oxygen is only responsible for the consumption of approximately half the hydrogen. The remainder of the hydrogen is lost by diffusion of either the hydrogen molecule or radical out of the flame, or through dissociation (Reaction [5]). Since diffusion is inversely proportional to the square root of the mass of the molecule or atom, the rates of diffusion for the hydrogen molecule and radical are

large. The loss of molecular hydrogen through Reaction [5] does not begin to be important until the temperature of the flame has increased above 2000 K.

$$H_2 + M \rightarrow 2H + M \qquad [5]$$

The relative unimportance of this reaction at low temperatures is understood when the rate constants for Reaction [5] at 600 and 2500 K are calculated to be $k_{600\ K} \approx 1.0 \times 10^{-35}$ $cm^6/sec\text{-}moles^2$, and $k_{2500\ K} \approx 9.0 \times 10^5$ $cm^6/sec\text{-}mole^2$. It is apparent that at low temperatures, Reaction [5] is very slow; only at high temperatures does the reaction begin to be important in the removal of hydrogen from the flame. Consumption of hydrogen by O_2, diffusion of hydrogen out of the flame, and thermal degradation of hydrogen through Reaction [5] contribute to loss of the molecular hydrogen Raman signal in the flame profile in Figure 7.

8. Results of Halon 1301 Inhibited H_2/O_2 Flame

The addition of 0.5 liters per minute of Halon 1301 (2.4 percent by volume) to the flame caused the luminous blue combustion zone of the flame to move visibly farther from the burner surface than observed for the normal flame. Four molecules were profiled in this flame: hydrogen, oxygen, Halon 1301 (at 758.5 cm^{-1}), and the C_2 radical (Reference 22). The C_2 concentration profile is measured from its fluorescence spectrum at 563.5 nm, and the profiles of the other species were determined from the Raman spectra. The C_2 fluorescence spectrum occurs when the 514.5-nm laser wavelength is used and is not present when the 488.0-nm laser wavelength is used. This is an expected result on the basis of previously reported experience.

The concentration profiles of these molecules and the temperature profile of the flame are presented in Figure 8, which illustrates the same height above the burner and has the same percent concentration scale as Figure 7 but a temperature range of only 1200 K rather than 3200 K.

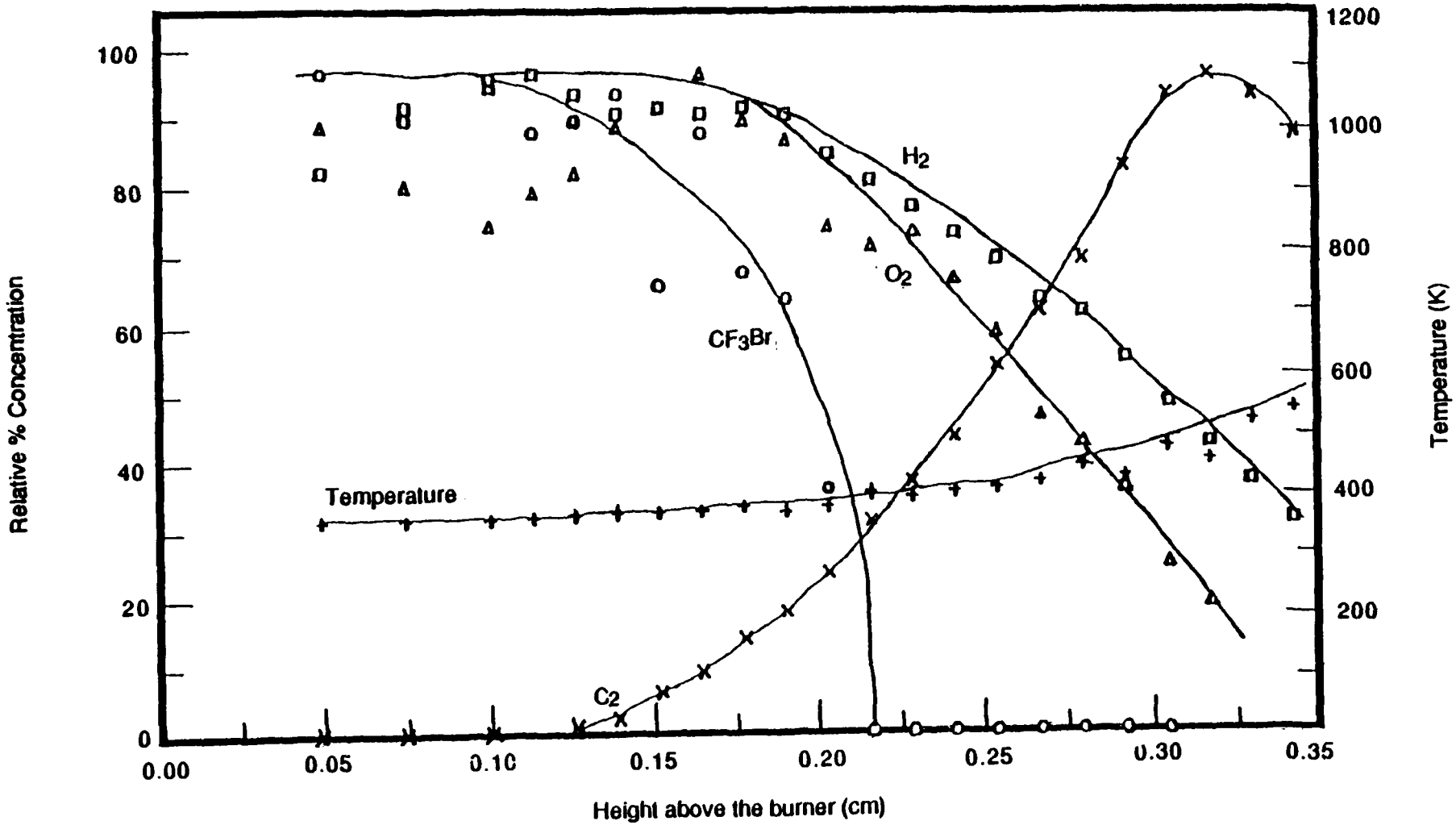


Figure 8. Concentration Profiles of Hydrogen, Oxygen, Halon 1301, and C_2, as well as the Temperature Profile for a Halon 1301 Inhibited Hydrogen/Oxygen Flame.

The profiles presented in Figure 8 confirm that the combustion zone has moved away from the burner surface. The figure also shows rapid destruction of Halon 1301, as indicated by both the rapid drop in the Halon 1301 concentration profile and the subsequent rise in the C_2 profile. The hydrogen and oxygen concentration profiles show a slow drop, and the temperature profile indicates that the area of the flame represented by the data is the precombustion zone. Figure 9 continues the temperature profile for the flame past 3.33 mm above the burner. The rapid rise in temperature that occurs after 3.33 mm above the burner indicates the onset of the combustion zone and shows that the data in Figure 8 represent the pre-combustion zone, which is the area of interest for this work. The final temperature of the inhibited flame could not be measured because the concentration of the hydrogen molecule fell below the level needed to produce an adequate Raman signal for the temperature measurement. Also of importance in Figure 8 is the absence of a concentration profile for water. Although attempts were made to detect water molecules, the presence of water could not be established in the investigated area of the flame.

9. Comparison of Normal and Inhibited Flames

Several differences can be seen in the comparison of the concentration profiles in Figures 7 and 8 for uninhibited H_2/O_2 and Halon 1301-inhibited H_2/O_2 flames.

a. The C_2 radical is present in the halon-inhibited flame and not in the normal flame. This is to be expected since the normal flame has no source of carbon atoms.

b. The onset of the combustion zone is farther from the burner surface for the inhibited flame than for the normal flame. This indicates that the burning velocity of the inhibited flame is slower than that of the normal flame.

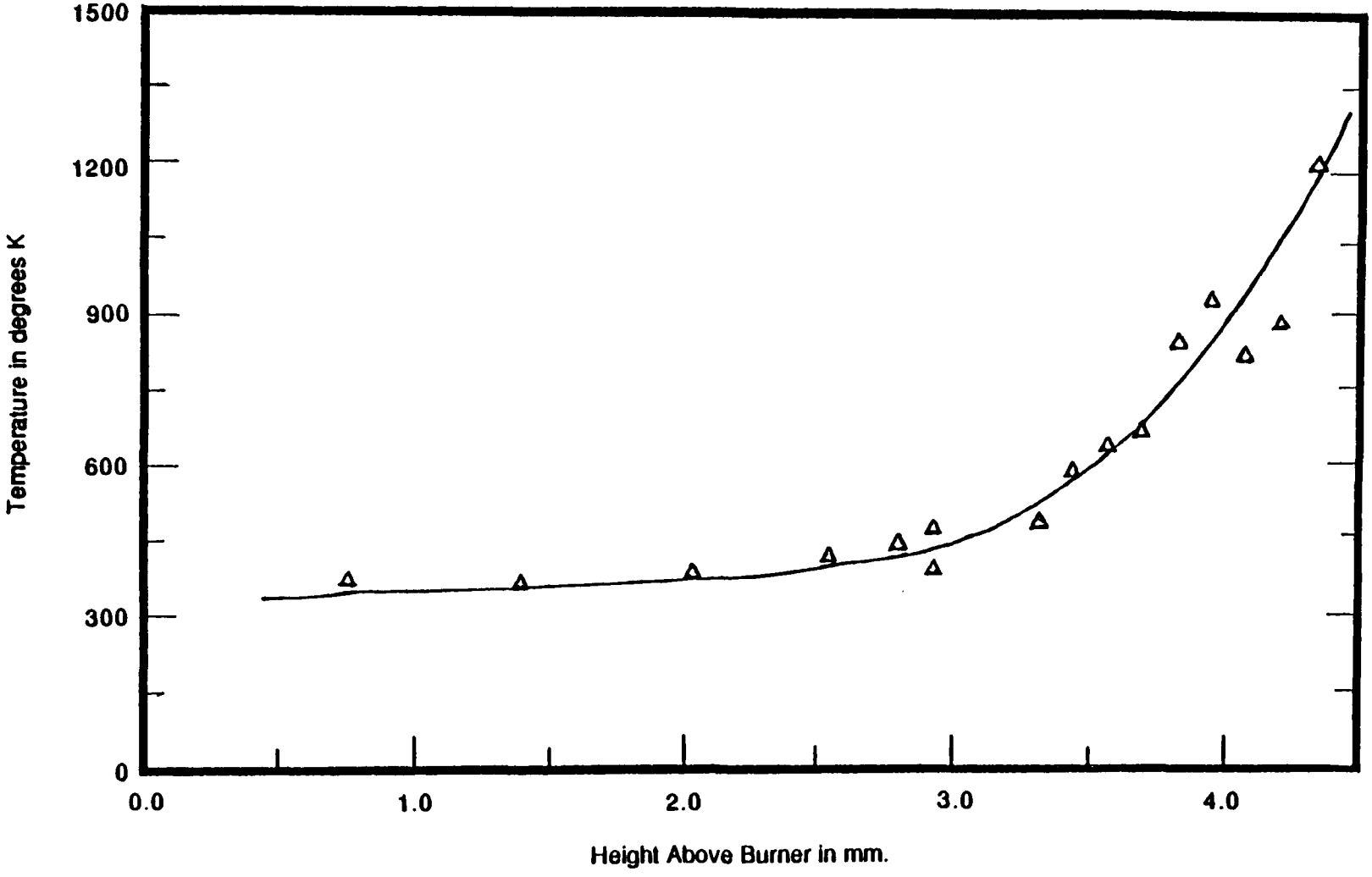


Figure 9. Temperature Profile of the Halon 1301 Inhibited Hydrogen/Oxygen Flame Showing the Temperature of the Flame Higher in the Flame.

c. Given that the combustion zones for the two flames occur at different heights above the flame, it is expected that the H_2/O_2 concentration profiles will differ, as they do.

d. Since the rate of change in the concentration of any flame species is proportional to the slope of its concentration profile at any position in the flame, comparison of the concentration profiles of oxygen and hydrogen for the two flames indicates that the rate at which these molecules are consumed is substantially reduced in the inhibited flame.

e. Although water is found in detectable amounts in the pre-combustion zone of the normal flame, none was detected in this same region for the inhibited flame.

f. The temperature profiles for the two flames are similar, with the profile for the inhibited flame reaching a maximum higher than that for the uninhibited flame. This is expected from the movement of the combustion zone described in b. above.

g. Both profiles of the species in each flame have a region where the oxygen and hydrogen concentrations are constant over several tenths of millimeters in the flame. This indicates that the profiles cover the warming zone of the flame, where few or no reactions are occurring.

Among the above differences in the profiles presented in Figures 7 and 8, the reduction in the rate of consumption of both hydrogen and oxygen and the lower burning velocity found for the inhibited flame are the most important. Other differences cannot be easily related to the chemical process occurring in the flame.

B. MATRIX ISOLATION SPECTROSCOPY

1. Introduction

Electric discharges have been used extensively as sources for radicals and ions. Microwave discharges have found especially wide application in this context, but DC discharges have also been used in some experiments. In principle, a DC discharge should offer the experimentalist greater flexibility in the design of an experiment. One can not only select the polarity of the discharge, but can also operate the discharge in a metal source. Microwave discharge experiments are usually constrained to employ tubes made of insulators such as quartz and alumina.

It was, therefore, of interest to explore in some detail the operating regimes for hollow cathode and hollow anode glow discharges. It was immediately found that satisfactory glow discharges could be sustained in aluminum electrodes with a pressure of a few torr of argon. Moreover, when the argon was seeded with a fraction of one percent of a halogenated hydrocarbon, the products were surprisingly similar to those one would expect to find in a flame seeded with the same halogenated compound. Thus, it soon became apparent that one might be able to explore much of the chemistry that is characteristic of flames by studying the reactions found in low pressure argon discharges seeded with fuels, oxidizers, and flame suppressants, especially Halons 1301, 1211, and 2402.

The matrix isolation technique is especially well suited for examining the products of such discharges. When the products of the discharge are condensed on a cold, infrared-transparent target, both the argon carrier gas and the product molecules, radicals, and ions condense on the target. Moreover, since the argon is present in great excess, the frozen argon matrix traps both the stable and unstable products of the discharge, prevents them from undergoing further reactions, and permits the characterization of these products spectroscopically using conventional Fourier Transform Infrared (FTIR) techniques.

2. Experimental

Figure 10 illustrates the principal components of the electric discharge supported flame system. The hollow electrode was fabricated of 1100 aluminum by boring a 2.44 mm (0.096-inch) diameter hole to a depth of 2.5 cm (1.0 inches). A 0.343 mm (0.0135-inch) diameter hole drilled in the closed end of the electrode served as the nozzle through which the discharge products were sprayed onto the cold target. The nominal length to diameter ratio of the nozzle was about 5. The coaxial counter electrode was fabricated from 0.79 mm (0.031 inch) diameter aluminum wire. Except for the last 2 mm, the counter electrode was sheathed in a high-purity, low-silicon alumina tube having a nominal outer diameter of 1.5 mm (0.063 inches).

Matrices were condensed on a cesium iodide target cooled by an Air Products Model DE202S Displex closed-cycle, variable-temperature cryostat capable of achieving a minimum temperature of about 10 K. The high vacuum for the cold cell was achieved with a 4-inch diffusion pump equipped with a liquid nitrogen-cooled chevron baffle and a liquid nitrogen-cooled U-trap. As is typical for such systems, traces of water, carbon dioxide, carbon monoxide and other hydrogen, oxygen, and nitrogen compounds were usually observed in the spectra of the discharge products.

In typical experiments, the optically transparent cesium iodide target was held at 10 K (nominally) throughout. The seed gas was mixed with argon in a molar ratio of one part seed gas to 1000 parts argon. The typical rate of deposit was about one millimole of argon per hour. While a majority of the experiments were performed with the hollow electrode as the negative electrode (hollow cathode), the polarity was reversed for several experiments. The experimental parameters for these latter, hollow anode, experiments were significantly different from those for the hollow cathode experiments. In the hollow cathode mode, a stable discharge could be maintained with a measured upstream pressure of 0.8 to 8.0 torr, a discharge voltage of 400 to 800 volts, and a discharge current of 0.1 to 8.0

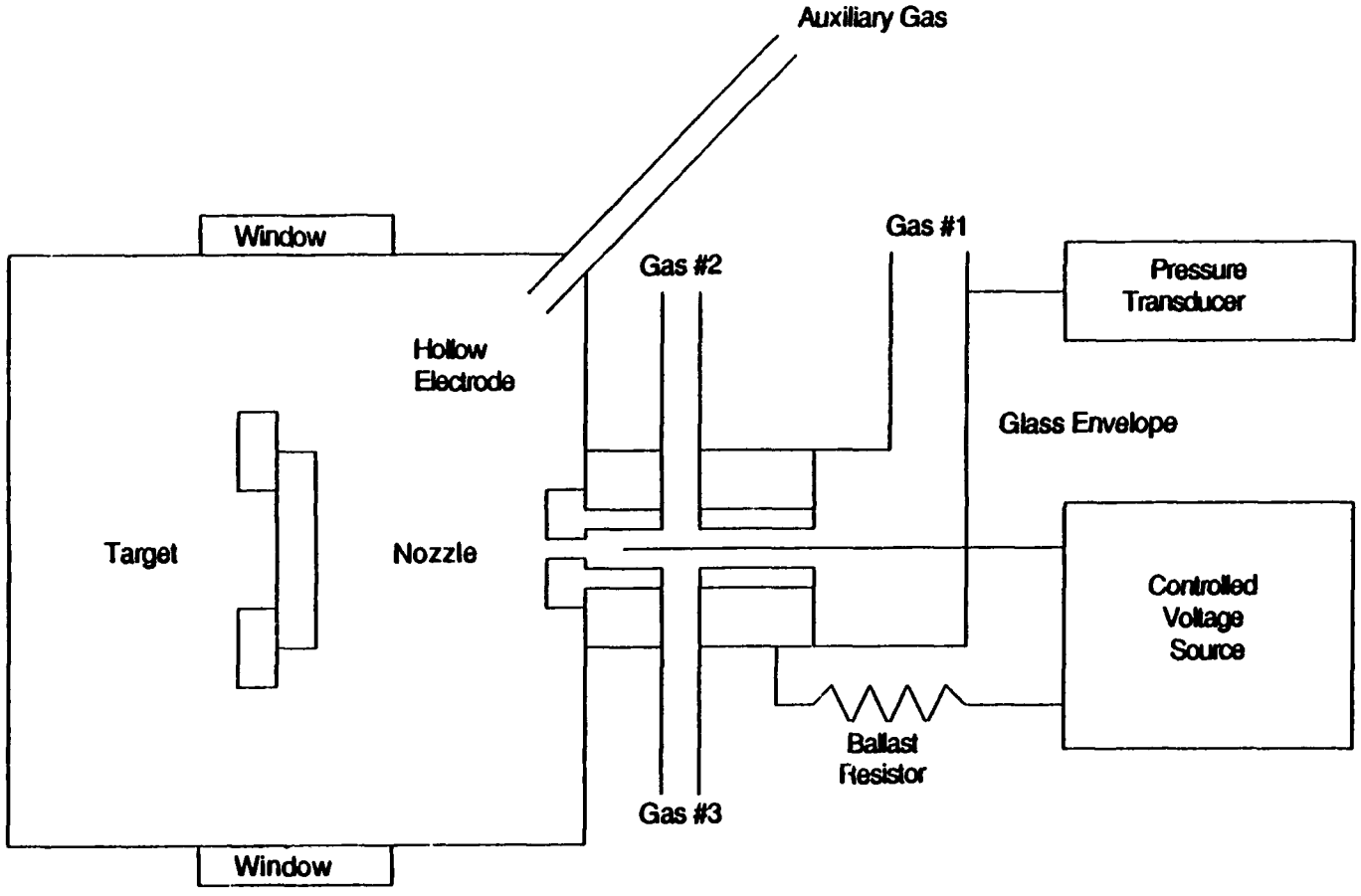


Figure 10. Principal Components of the Electric Discharge Supported Flame System. Block diagram of the triplex discharge cell.

milliamps. By contrast, the hollow anode discharge required a higher pressure and was sustained at a much lower current. For the latter experiments, the useful pressure range was 5 to 7 torr, the voltage could be varied from 400 to 600 volts, and the measured current was 0.02 to 0.47 milliamp.

The spectra were recorded from 4000 to 400 cm^{-1} with a Nicolet 6000C FT-IR Spectrophotometer using a liquid nitrogen-cooled, mercury-cadmium-teluride (MCT) detector at a resolution of 1 cm^{-1}.

3. Results

A total of 28 experiments were performed: 13 with Halon 1301, 12 with Halon 1211, and 3 with Halon 2402. The experiments can be conveniently divided into three groups. In the first group, the argon-halon mixture was simply passed through the discharge. In a second set of experiments, a small amount of hydrogen or oxygen was added to the argon halon mixture. The third set of experiments used vacuum ultraviolet (VUV) photolysis (in place of the electric discharge) to generate the product species.

a. Discharge Experiments

The purpose of the simple discharge experiments was to characterize the fragmentation patterns of the various halons. The dilute argon-halon mixtures were passed through the discharge, the products were collected in the frozen argon, and the spectra were recorded. With almost no exceptions, the expected fragments were observed: CF, CF_2, and CF_3. A variety of stable molecules were also observed. These included C_2F_4 (probably from recombination to two CF_2 radicals), CF_4 (also from a recombination reaction), HF (from traces of water in the system), HCF_3 (also from reaction with water), and OCF_2 (perhaps from reaction of F atoms with CO or CO_2 impurities). In addition to the radicals and stable molecules, several ions were also observed in deposits generated by hollow cathode (but

not hollow anode) discharges. The appearance of these ions led to the series of photolysis experiments (described below).

An interesting aspect of discharges in Halon 2402 was the appearance of CF_3Br (Halon 1301) as a discharge product. The formation of CF_3Br provides additional evidence that considerable complex chemistry occurs in the discharge and subsequently in the matrix.

Perhaps the most noteworthy feature of the discharge experiments was the fact that the same fragments and stable species were also observed in flames into which halons have been introduced. This observation immediately suggested that it might be possible to gain insight into the behavior of typical flames by studying their electric discharge-supported counterparts, which in turn led to the next set of experiments, in which both hydrogen and oxygen were intentionally added to the argon-halon mixture in the hollow electrode.

b. Hydrogen and Oxygen Doped Discharges

In five experiments, varying amounts of hydrogen were added to a mixture of argon and Halon 1301, and the combined mixture was passed through the discharge. Data from one of these experiments are displayed in Figure 11. In the experiment illustrated by this figure, the amount of hydrogen increased from experiments 1 to 9. The data indicate that the relative amount of CF_3 decreased as the amount of hydrogen was increased; they further suggest that the hydrogen reacted with the CF_3 (either F-atom abstraction by H atoms or molecules, or recombination of CF_3 with H atoms to form HCF_3). Note, however, that this experiment was not repeated. The results must be treated very cautiously and should be considered only suggestive at this point.

When hydrogen was added to the argon-CF_2BrCl mixture, the dominant hydrogen halide was HCl; only a trace of HF was observed, and no

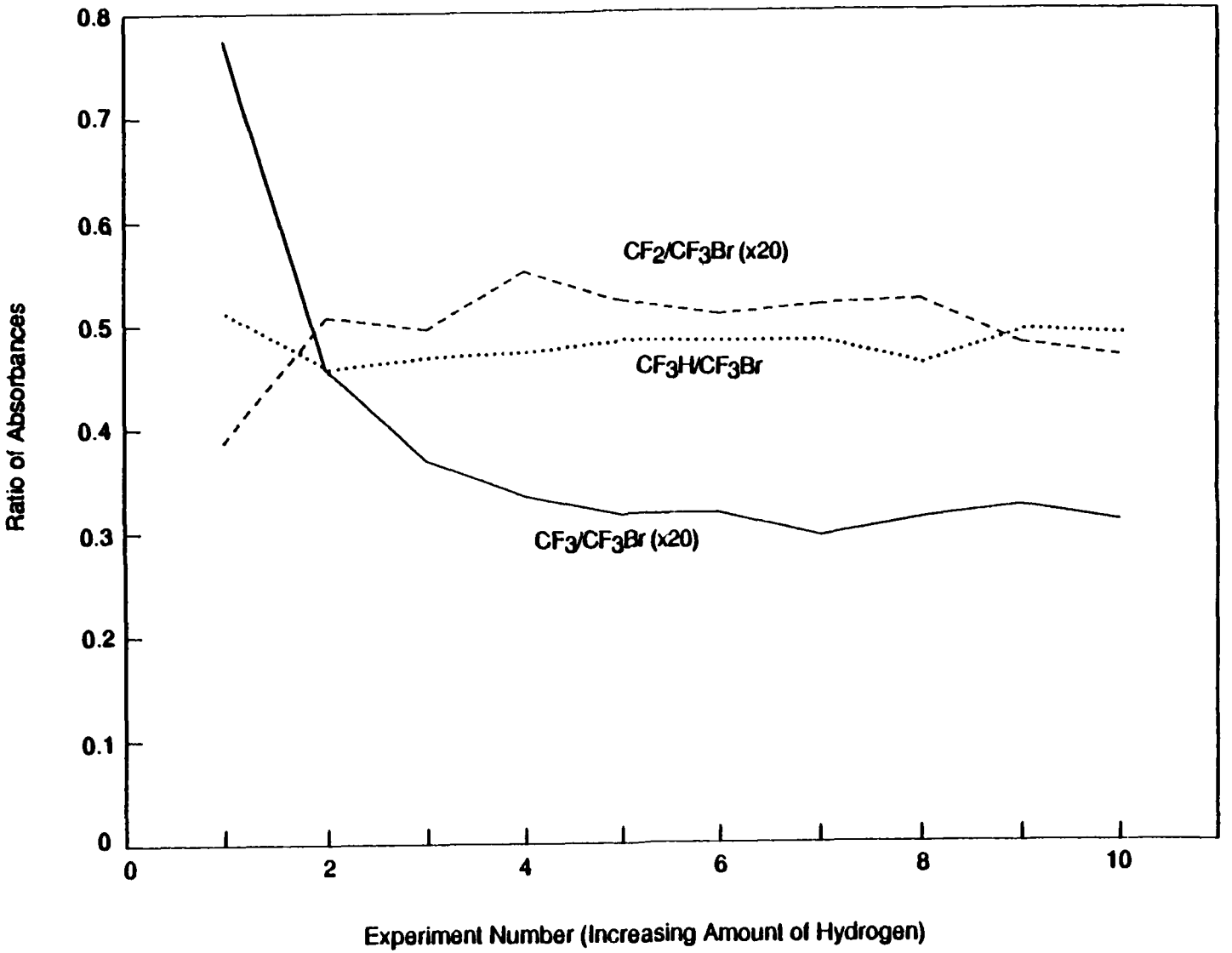


Figure 11. Data from Passing a Mixture of Argon, Halon 1301, and Varying Amounts of Hydrogen Through an Electric Discharge. Ratios of CF_3H, CF_3 and CF_2 to CF_3Br as a function of amount of hydrogen added.

HBr was found. This result can be understood by considering the following set of reactions.

$$CF_2BrCl + H \rightarrow HBr + CF_2Cl, \quad \Delta H(298\ K) = -74\ kJ \qquad [6]$$

$$CF_2BrCl + H \rightarrow HF + CFBrCl, \quad \Delta H(298\ K) = -131\ kJ \qquad [7]$$

$$CF_2BrCl + H \rightarrow HCl + CF_2Br, \quad \Delta H(298\ K) = -202\ kJ \qquad [8]$$

As indicated by these reactions, the thermodynamically favored reaction yields HCl. The observation of the thermodynamically favored product to the exclusion of the less favored hydrogen halides strongly suggests that thermodynamic equilibrium is achieved in the electric discharge-supported flames. It should be noted in passing that HCl is a sink for H and Cl atoms, while the Br atoms in HBr are still available to participate in the catalytic recombination of H atoms.

The addition of oxygen to the argon-Halon 1301 mixture yielded no obvious changes in the pattern of discharge products.

c. Photolysis Experiments

In the photolysis experiments, the argon-halon mixture was introduced into the cold cell through a separate spray-on line (without being passed through the discharge), and pure argon was passed through the discharge to serve as a vacuum ultraviolet (VUV) photolysis source. With this configuration, the only observed reactions are those due to the interaction of the photons from the argon discharge (especially the Ar resonance lines at 104.8 and 106.7 nm) with the halon molecule. In the case of Halon 1301, both the positively and negatively charged parent ions (CF_3Br^+ and CF_3Br^-) were observed. Halon 1211 displayed much more photolytic activity than did Halon 1301. In addition to previously identified ions (CF_2BrCl^-, CF_2Br^-, CF_2Br^+, and CF_2Cl^+), the two ions CF_2BrCl^+ and CF_2Cl^- were apparently observed for the first time.

C. PHOTOIONIZATION MASS SPECTROMETRY

1. Purpose

The purpose of these experiments was to conduct a set of static gas tests in which the flame free radicals H, O, and OH were generated by photolysis of the appropriate precursor in the presence of a halon. The intent is to arrest the typical flame reactions immediately after the initial reactions occur rather than allowing reactions to proceed to the thermodynamic products. Various analytical techniques were used to identify primary reaction products of halon free radical reactions.

2. Experimental

The bulb experiments were conducted in a 1.4 liter stainless steel chamber equipped with a quartz window that passed UV radiation down to 1750 Angstroms. The chamber could be evacuated to a pressure of 10^{-3} torr and an inlet manifold permitted introduction of gases as required. The pressure was monitored with a capacitance manometer. The entire chamber was wrapped with heating tape and could be warmed to temperatures above ambient. All seals were made with metal gaskets so that adventitious organic molecules could be removed by degassing at elevated temperatures. Light sources used to irradiate samples in the chamber consisted of the outputs of a XeCl excimer laser at 3080 Å and of a high-pressure xenon arc lamp, which gives a spectral output similar to that of the sun as it irradiates the stratosphere. Light from the xenon arc lamp was coarsely focused on the inside of the chamber by means of a quartz lens arrangement.

After irradiation, the products were collected by trapping the entire contents of the chamber in 1-liter, stainless steel sample containers cooled by liquid nitrogen. Samples were removed from these bottles as needed. These containers served as long-term storage chambers for the product mixtures. For gas chromatography/mass spectrometry (GS/MS) analysis, small samples were collected in vials capped with rubber septa;

gas-tight syringes were used to transfer samples to the GC/MS. Samples were transferred to 10-cm gas cells under controlled pressures (on a vacuum line) for the Fourier-transform infrared spectroscopy (FTIR) studies.

In a typical experiment, the reaction chamber was charged to 10 torr with the radical precursor HI and brought to a final pressure of 720 torr with Halon 1301 (CF_3Br). The chamber was stirred at room temperature while irradiated by the weakly focused light from a 750-watt xenon arc lamp for 22 hours. The product charge was transferred to the 1-liter holding vessel by immersing the holding vessel container in liquid nitrogen until condensation of the product vapor was complete, as indicated by the pressure in the reaction chamber. A small sample was later injected into a Finnigan GC/MS with a 30-meter glass capillary column; the mass spectra of the peaks exiting the column were recorded.

Some reactions were conducted at elevated temperatures. In these cases, the reaction vessel was wrapped with heating tape and covered with aluminum foil. The chamber was heated until an internal thermocouple indicated a temperature of 373 K. At this time the xenon lamp was turned on, and the sample was irradiated for 22 hours.

3. Results

The list of experiments conducted is given in Table 2. As can be seen from Table 2, only one experiment was run with the XeCl laser source. This run was analyzed by GC/MS, and no evidence of decomposition products could be seen. The decision was, therefore, made to use a source with a higher flux at shorter wavelengths. The laser was run at 30 Hz for 5 hours. Although the number of photons per pulse is very high, about 10^{12}, the pulses have a width of only 4 ns, and the total exposure time of the sample at 308 nm is only 0.12 μs. This, combined with the low cross section for dissociation at 308 nm, makes the laser experiment impractical unless optics are constructed so multiphoton dissociation or ionization is possible. In

TABLE 2. PHOTOLYSIS EXPERIMENTS OF HALONS 1211 AND 1301 WITH FREE RADICAL PRECURSORS.

Halon	Precursor	Free radical	Source	T, K.
1211	CH_2O	H	XeCl laser	298
	CH_2O	H	Xe lamp	298
	CH_2O	H	"	373
	HI	H	"	298
	HI	H	"	373
	O_2	O	"	298
	NO_2	O	"	298
	NO_2	O	"	373
1301	O_2	O	"	298

the present case, it was more expedient to use the intense Xe arc lamp that is rich in short wavelength radiation. The total pressure in the reaction chamber increased faster at 373 K than it did at 298 K. As discussed below, this may have significant mechanistic implications.

The GC/MS results are ambiguous. Extensive analyses of product gases from all of the experiments were carried out by GC/MS using a range of GC column temperatures, carrier gas flow rates, ionization conditions, and background pressures. Clean separation of the low molecular weight products from one another and from the dominant peaks due to unreacted starting materials was not realized. Longer exposure times were deemed unreasonable because of the ever-increasing possibility of secondary photolysis reactions. By careful manipulation of the sampling interval of the peaks emerging from the GC column, it was possible to identify small amounts of

products of free-radical reactions with halons. Unfortunately, these could not be quantified because the apparent amounts of products are sharply dependent on precise reproducibility of the sampling period of the GC peak. Such reproducibility of the sampling period was impractical. Fundamentally, the approach is sound; a different sample analysis protocol is needed.

Nevertheless, in all of the cases of photolysis with the xenon arc lamp, evidence of small amounts of products was seen. In every case, C_2F_4 was observed. When the precursor (CH_2O or HI) yielded H on photolysis, small amounts of HBr could be seen in the mass spectrum. No oxygenated products of reactions of O with halon could be clearly identified when the precursor was O_2 or NO_2 even though some C_2F_4 was found. In all cases, other peaks were found in the mass spectrum of products that were not found in that of the starting materials, but these were too faint and irregular to be satisfactorily identified. This, again, is due to the particular GC/MS used and not to a fundamental limitation of the method.

FTIR spectra were taken of the products of photolysis of Halon 1211 with NO_2 and of Halon 1301 with O_2. In both cases, only peaks due to reactants were seen since they dominated the spectrum. The sensitivity of the FTIR is simply not great enough to allow identification of the products without prior concentration procedures. Some small features can be seen in the spectra, but they cannot be extracted from the noise. As discussed above, longer exposure times defeat the purpose of isolating initial reaction products.

No differences in reaction products could be discerned for the higher temperature experiments in spite of the fact that a greater pressure change was observed here than at lower temperatures. Unfortunately, one cannot state unambiguously that the reactions were more extensive at elevated temperatures.

SECTION IV

RECOMMENDATIONS AND CONCLUSIONS

A. LASER RAMAN SPECTROSCOPY

In order to identify the mechanism by which Halon 1301 inhibited the H_2/O_2 flame, the flame profiles for both the normal and inhibited flame must be interpreted. Of importance to the interpretation of the concentration profiles is the relationship between the slope of these profiles and the reaction rates of the molecules represented by them. This relationship comes about as a result of the flow of the gas upward through the flame. For a uniform, nonturbulent flow of the gases, the velocity is dz/dt, where z = distance, t = time, and the slopes of the concentration profiles in Figures 7 and 8 are d[conc.]/dz. The relationships between the slopes of the concentration profiles and the reaction rates of the molecules represented by the profiles are

$$d[conc.]/dz \cdot dz/dt = d[conc.]/dt \qquad (8)$$

Therefore, in each case, d[conc.]/dz is proportional to d[conc.]/dt. This relationship is important because it demonstrates that the concentration profiles in Figures 7 and 8 are useful in the interpretation of the rate processes of the flame.

Examination of the concentration profiles of the inhibited flame shows the CF_3Br molecule is the first to begin decomposing; therefore, the first effect of the addition of the halon to a normal flame is the scavenging of thermal energy. This scavenging, however, is expected to have little effect on the flame, since the amount of CF_3Br added to the flame is small, approximately 2 percent by volume. Next, it is expected that the Br radical will be the first radical liberated by the decomposition of Halon 1301. Bromine will detach preferentially from the CF_3Br molecule because the C-Br

bond energy is approximately 55 kcal per mole less than the C-F bond energy (Reference 23). Consequently, bromine atoms are the first radicals to occur in the flame. An exhaustive search for the electronic Raman spectrum of the bromine radical in the flame was not successful, no doubt because of its low concentration of less than 2 percent by volume and the lower intensity of atomic electronic Raman transitions compared to vibrational Raman transitions (References 24 and 25). The concentration of Br radicals cannot exceed the concentration of Halon 1301 added to the flame. In fact, it is expected to be considerably less as a result of reactions with other molecules in the flame. Although the bromine radicals were undetected, their presence early in the flame is a likely explanation of the Halon 1301 concentration profile.

The C_2 concentration profile confirms and matches the CF_3Br profile well, which implies the release of fluorine radicals into the flame. In this case, the search for fluorine radicals was not carried out, since the intensity of the Raman spectrum from fluorine radicals is expected to be even smaller than that for the undetected bromine radical. It is important, however, to note that the fluorine radicals also arise early in the flame and, therefore, may play a part in the inhibition processes.

The molecular hydrogen concentration drops slower in the inhibited flame than in the normal flame by a factor of about 2.3; therefore, the net rate of disappearance of H_2 must be slowed by a similar amount. The major reaction involved in the destruction of H_2 is the elementary process shown in Reaction [9].

$$O + H_2 \rightarrow OH + H \qquad [9]$$

for which a simple rate law (Equation 9) can be written:

$$d[H_2]/dt = -k_{H_2}[O][H_2] \qquad (9)$$

Here $[H_2]$ and [O] are the concentrations of these species, and t is time. From Equation (9) it is evident that the rate of destruction of H_2 depends on its own concentration multiplied by that of the oxygen radical.

Clearly the role of atomic oxygen is important in sustaining and propagating combustion. Since O is not supplied to the flame, as are the starting reactants H_2 and O_2, it must be produced in the flame. The question arises as to which reactions in a normal flame are responsible for the production of oxygen radicals and how these reactions might be affected by the addition of Br and F. Only the Br and F radicals are considered because the flame profiles for C_2 suggest that little to no CF_x radical is present during H_2 consumption.

For normal combustion, Reaction [10] is known to dominate all other reactions involving the concentration of O, except Reaction [9] (References 26-28).

$$H + O_2 \rightarrow OH + O \qquad [10]$$

Also, no reactions of O with Br and F can compete with Reaction [10] for the oxygen radical (References 26, 29, 30). Changes in the rate of Reaction [9] must be the cause of changes in the O concentration in the flame. A rate equation for Reaction [10] is

$$d[O]/dt = k_o[H][O_2] \qquad (10)$$

Reaction [10] and [9] rapidly lead to an effective equilibrium of the three free radicals O, H, and OH in a flame. As a consequence, any reactions of H with either Br or F will have their effects propagated to the concentrations of the O and OH free radicals as well.

Both Br and F react with atomic hydrogen to form compounds with large dissociation energies. For example, Br traps atomic hydrogen by

recombination in the well-established HBr catalytic cycle (Reactions [11], [4], and [12]) that occurs at a rate fast enough to compete with Reaction [10] for H (References 26, 29, 30).

$$Br + Br \rightarrow Br_2 \quad [11]$$
$$H + Br_2 \rightarrow HBr + Br \quad [4]$$
$$H + HBr \rightarrow H_2 + Br \quad [12]$$
$$\overline{H + H \rightarrow H_2} \quad [13]$$

The rate constants for Reactions [10], [4], and [12] are calculated using data from Reference 28 to be 8.56×10^{10}, 6.23×10^{13}, and 7.32×10^{12} cm^3/mole-sec, respectively. These values are obtained from the table in Reference 28 using the Arrhenius equation (11).

$$k = A \exp(-E_a/k_b T) \quad (11)$$

where k is the rate constant, A is the Arrhenius (pre-exponential) factor, E_a is the activation energy of the reaction, k_b is Boltzmann's constant, and T is the absolute temperature. The ability of Reactions [4], [12], and [13] to compete with Reaction [10] is apparent from these rate constants. The larger rate coefficients for Reactions [4] and [12] mean that Br_2 and HBr compete favorably with O_2 to interfere with the chain-branching process that supports combustion.

Since Br has an effect on Reaction [10], the question arises whether F might have a similar effect on this reaction. If fluorine replaces bromine in Reactions [11], [4], and [12], the new reactions would be

$$F + F \rightarrow F_2 \quad [14]$$
$$H + F_2 \rightarrow HF + F \quad [15]$$
$$H + HF \rightarrow H_2 + F \quad [16]$$

In this case, the net rate of the recombination of the hydrogen atoms to the hydrogen molecule is slow. The limiting step is Reaction [16] for which the rate constant is 112 cm^3/mole-sec compared to the rate constant of 7.32 x 10^{12} cm^3/mole-sec for Reaction [12]. The dramatic difference in the reaction rates is due to the greater stability of the HF molecule, which has a bond strength of 135.9 kcals per mole, compared to the HBr molecule, which has a bond strength of 87.4 kcals per mole (Reference 26). The result is that no HF catalytic cycle exists to influence the concentration of the hydrogen radical. In the removal of hydrogen atoms by reaction with F through Reaction [17], it should be noted that this reaction can only be responsible for a small amount (about 3 percent) of the loss of the hydrogen radical.

$$H + F + M \rightarrow HF + M \qquad [17]$$

In this interpretation, the HBr catalytic mechanism is the most likely pathway for decreases in the hydrogen and oxygen radical concentrations in the flame. Problematic is the fact that although the presence of HBr in the flame is assumed by the HBr mechanism, none could be detected in the flame. One reason for not detecting HBr is its anticipated low concentration of less than 2 percent by volume. Attempts to increase the concentration of HBr in the flame by reducing the H_2 and O_2 flow rates or by increasing the CF_3Br concentration caused the flame to move out of the laminar flow region and become turbulent. HBr was still not detected in the flame, a result most likely due to the increased noise associated with turbulent flames. Similar results were found when searching for the bromine molecule.

Despite the fact that neither HBr nor Br_2 was detected in the flame, inferences may be drawn from both the oxygen and hydrogen concentration profiles. Figures 7 and 8 show that the rate at which oxygen is removed from the inhibited flame is substantially reduced compared to the rate for the normal flame. Since Reaction [10] is principally responsible for the destruction of O_2 (by reaction with hydrogen radicals), some other reaction may cause the removal of the hydrogen radicals from the flame. According to

Reactions [11], [4], and [12], these hydrogen radicals recombine to form H_2. This recombination causes a reduction in the rate of loss of H_2 and, consequently, reduces the rate at which hydrogen is removed from the flame. This assumption is consistent with the observations in Figures 7 and 8.

The trends for the concentration profiles shown in Figures 7 and 8 are the early loss of the Halon 1301 and the concomitant rise in the C_2 concentration. The mechanism by which these two changes are coupled so closely in time is not obvious; however, these observations require that CF_3Br decomposition and probably the generation of bromine and fluorine radicals occur early in the flame, in fact before H_2 or O_2 decomposition. When Halon 1301 is added, the oxygen and hydrogen concentration profiles show decreases in the rates of decomposition.

Laser Raman spectroscopy of hydrogen/oxygen flames extinguished with halon provides excellent identification of the principal flame species; however, it is difficult to detect minor species present in low concentrations. Thus, although a large amount of useful data may be generated from these laser Raman spectroscopy studies, it is believed that other experimental procedures, as described below, will provide more useful data in the detailed Phase III studies.

Over the past 8 to 10 years, a vast amount of knowledge has been gained in the understanding of the chemical and physical processes governing combustion. Most important to this work has been the advent of the computer modeling of combustion. Although modeling techniques have accurately described many combustion processes, these techniques still rely on information gathered through experimentation. Therefore, in order to continue the development of these computer modeling programs and further the understanding of the fundamentals of combustion, more work, similar to that presented in this report, needs to be performed (References 26, 29, 30).

The data presented here add needed confirmation of the presently accepted chemical mechanism for halon inhibition. Most significant is the

fact that the information is derived from studies of an atmospheric flame, for which little data had been previously acquired, despite the fact that combustion normally occurs at atmospheric pressures.

The HBr-catalyzed recombination of hydrogen radicals to form hydrogen molecules accounts for many of the differences observed in this work between the normal and inhibited H_2/O_2 flames. Further studies, using different methods or higher intensity pulsed lasers and more sensitive detection devices than those used here are necessary in order to detect more of the chemical species occurring in halon-inhibited flames.

B. MATRIX ISOLATION SPECTROSCOPY

While much work remains to be done, electric discharge supported flames and matrix isolation spectroscopy have considerable potential for exploration of the interactions of fire suppressants with flames. It may be worthwhile to pursue the interaction of CF_x radicals with H atoms and H_2. However, the greater payoff will probably result from exploration of other fire suppression systems that are not as thoroughly characterized. Despite the utility of the matrix isolation-FTIR technique, it has been ruled out as the major approach in the present study, based on timeliness and cost effectiveness. Photoionization mass spectrometry is favored.

C. PHOTOIONIZATION MASS SPECTROSCOPY

Two important lessons can be learned from these experiments. First, Halon 1211 does react with the free radical H, but the cross section of the overall process is small. Hence, a highly sensitive analytical method such as mass spectrometry is necessary to identify the initial reaction products and to locate transient intermediates. Second, no evidence, under our conditions, was found for reactions between O atoms produced by photolysis of O_2 or NO_2 and either Halon 1211 or 1301. If this lack of reactivity with atomic oxygen is substantiated, it has significant implications for the

flame extinguishment mechanism. Note that this result was also found in the matrix isolation experiment.

The gas pressure in the reaction vessel increased more rapidly at 373 K than at 298 K, although no obvious parallel increase in the amount of product due to reaction with the halon was observed. The reaction rate, therefore, could be sharply dependent on the internal energy content of the halon, or the pressure increase could result from more extensive decomposition of the chromophore when vibrationally excited. The inability to make reliable concentration measurements does not permit distinguishing between these alternatives.

More extended photolysis periods could have been tolerated since the yield of reaction products was small and since no evidence of secondary reactions was found. The conditions of this experiment are vastly different from those which led Creitz (Reference 7), Larsen (Reference 27), and others to propose that halons work by trapping the flame free radicals H, O, and OH. The present conditions were specifically selected to generate very small amounts of product to reflect accurately the character of the initial reactions. The results hint that the mechanism may be more complex than previously supposed. Therefore, much more extensive experimentation under single collision conditions is necessary. Preliminary results will be discussed in the Phase III report.

Photoionization mass spectroscopy of the products of reactions has been shown to be the most cost-effective technique for continued studies of reactions of free radicals with halons. It offers the requisite analytical sensitivity and versatility for the critic l experiments.

SECTION V

EXPERIMENTAL PLAN FOR PHASE III

The conclusion of this survey study of several candidate methods for examining the nature of initial reactions is that the technique of photoionization mass spectrometry possesses both the capability of arresting reactions between halons and the flame free radicals and a sensitivity adequate to detect very small amounts of products. It is reasonable then to plan that in Phase III of this project at least one system involving a halon molecule and a free radical precursor be studied in depth.

Specifically, the bulb experiments point to unusual behavior of CF_2BrCl and the O atom sources O_2 and NO_2, in that no oxygenated fragments were found. Past experience shows that O_2 forms a complex with C_6H_6 and C_6F_6 and gives oxygenated fragment ions $C_6H_6O^+$ and $C_6F_6O^+$ of both substrates. In addition, it is known that an oxygenated fragment ion, ArO^+, can be formed from the very weakly bound complex $Ar \cdot O_2$. If no oxygenated complex ions are formed on dissociative photoionization of $CF_3Br \cdot O_2$, it would be a mechanistically significant result.

Halon 1301 was chosen for the Phase III experiments largely because it has a high vapor pressure at room temperature, the mass spectrum is very straightforward to interpret, and any dissociative photoionization fragments containing bromine can be identified readily by the characteristic bromine isotope signature in the mass spectrum. Any halon containing both bromine and chlorine will have a much more complicated mass spectrum. This type of spectrum is undesirable, for the initial experiments in which it is expected that a careful search for low number density products must be conducted. The mass spectra of otner halogenated compounds will in general be more complex than that of Halon 1301; however, the results with Halon 1301 will provide guidance in the interpretation of these more complex spectra.

It is expected that there will be no difficulty in extending the experimental technique to other halons eventually. Other analogous experiments have been performed by these investigators using materials with vapor pressures as low as 20 torr. The wide range of vapor pressures accepted by this technique indicates that it can be used on a wide variety of halocarbons.

Phase III will include the following:

1. Preparation of CF_3Br and O_2 mixtures in stainless steel cylinders in various proportions.

2. A study of the pressure dependence of the mass spectrum of these mixtures when expanded through a supersonic nozzle and ionized by 584-Å light using the UNM apparatus.

3. Analysis of these results to determine conditions under which predominantly dimers, $CF_3Br \cdot O_2$, are generated.

4. Design and construction of an ion kinetic energy analyzer for the quadrupole mass spectrometer.

5. A complete study of the optimized $CF_3Br + O_2$ mixture by dissociative photoioniztaion using the tunable VUV source, the 750 Mev synchrotron, at Brookhaven National Laboratory.

6. Analysis of the results and recommendations for future work.

APPENDIX A

DATABASE OF FIRE SUPPRESSION INFORMATION ON HALOCARBONS

SECTION I
INTRODUCTION

A. BACKGROUND

Under a United States Air Force contract, the New Mexico Engineering Research Institute (NMERI), Center for Technologies to Protect Stratospheric Ozone, of the University of New Mexico, is creating an extensive database as part of a program to develop halon alternatives (Reference 5). At present, the majority of the database is physical and chemical property data; however, toxicity, safety, literature, environmental, and laboratory data fields on more than 600 halocarbons are also included. These compounds include all acyclic chlorofluorocarbons (CFCs), hydrochlorofluorocarbons (HCFCs), hydro- fluorocarbons (HFCs), bromofluorocarbons (BFCs), hydrobromofluorocarbons (HBFCs), bromochlofluorocarbons (BCFCs), and hydrobromochlorofluorocarbons (HBCFCs), which contain one, two, and three carbon atoms. In addition, all perfluorocarbons (FCs) through perfluoroheptane and selected cycloalkanes are included. Also, information on a limited number of iodinated compounds has been collected.

Other databases being developed contain compilations of data for oxygen-substituted halocarbons and for non-halocarbon materials. The latter database is for materials other than halocarbons that have been shown to have flame suppressant capabilities. Neither of these other chemical compound databases is discussed further in this report.

This report discusses the improvement and expansion of the NMERI HALOCARBON DATABASE to include literature citation storage and retrieval capability. An expanded literature search related to fire suppression characteristic of halogenated aliphatic hydrocarbon was conducted. The resulting reference citations are included in a multirelational database, and copies of the papers, articles, and books in the database are stored at the site where halon alternative research is being performed.

The following is a summary of the fire suppression literature portion of the NMERI HALOCARBON DATABASE Version 2.0, including data fields, usage, and input and output screens. Version 2.0, an expansion of Version 1.0, contains additional physical property data; the physical/chemical properties, literature, laboratory, and toxicity information available for the compounds of interest has been integrated into a single multiuser, relational database.

The NMERI HALOCARBON DATABASE (Ver. 2.0) fire suppression literature collection contains reference citation information. The entire reference collection includes available research data, flammability, suppression/combustion characteristics, effects on the environment, firefighter safety, and toxicity related to the halocarbons of interest in the current AFESC/NMERI halon research effort.

Although the database has been developed, data input and format design continue. The work accomplished under the present project incorporated the literature database into the NMERI HALOCARBON DATABASE structure (Figure A-1) and provided a technology review of the fire suppression and combustion literature.

B. APPROACH

The NMERI HALOCARBON DATABASE (Ver. 2.0) consists of five major features: (1) a multirecord relational database; (2) continuous data acquisition and input with references; (3) estimation procedures for physical and chemical properties, ozone depletion potentials (ODPs), and global warming potentials (GWPs) for compounds with no reported values in the literature; (4) assurance of easy access and searching capability to database information; and (5) custom designed and standard report format capabilities.

The fully integrated database concept (Ver. 2.0) is illustrated in Figure A-1. The database provides an extremely powerful tool for the evaluation of halogenated hydrocarbons as alternative firefighting agents.

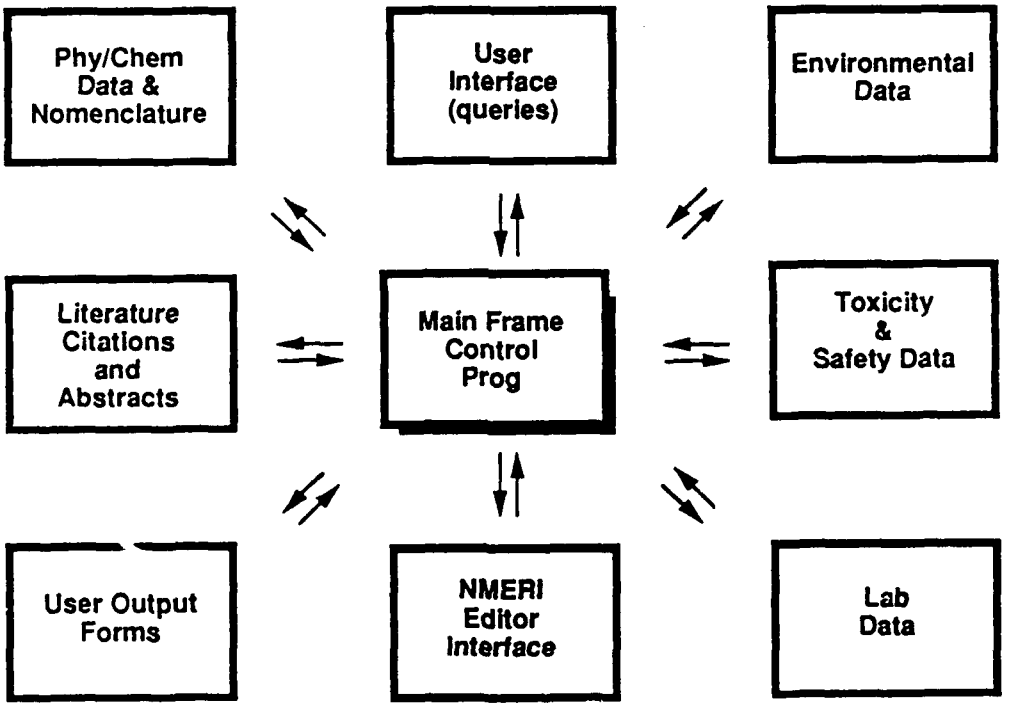


Figure A-1. NMERI HALOCARBON DATABASE Structure Version 2.0.

SECTION II
DATABASE

A. NMERI HALOCARBON DATABASE CONFIGURATION

The NMERI HALOCARBON DATABASE covers available chemical, physical, and environmental properties including safety and toxicological (inhalation and contact) information (Reference 5). Performance data derived from preliminary screening procedures and criteria are also included; these include fire suppression efficiency, ozone depletion potentials (ODPs), global warming potentials (GWPs), and fire suppression concentration test data. Algorithms to estimate physical and chemical properties for compounds with no reported values in the literature are also being developed for the database. All data compiled into the NMERI HALOCARBON DATABASE are referenced. The reference citation literature portion of the database was developed under the project, Initial Fire Suppression Reactions of Halons Phase II: Verification of Experimental Approach and Initial Studies (Reference 2).

The NMERI HALOCARBON DATABASE is being developed on a Harris HCX-9 main frame computer system (Reference 31), with a UNIX System V operating system, using a commercial relational database software package called Unify (Ver. 2.0) (Reference 32). The PC/desktop version of Unify is compatible with the main frame version; after the database structure has been created and information entered, updated floppy disk copies of the NMERI HALOCARBON DATABASE will be available for distribution to other interested researchers on a periodic basis. Convenient access to the replacement candidate information is guaranteed. The main frame allows faster, more powerful computing capabilities and permits all researchers immediate access to the most current information through telephone modem.

B. LITERATURE DATABASE

No general database of fire extinguishing agent literature existed before this effort. Such a database is essential for an effective and efficient program for developing new clean fire suppressants. All compound properties and other information included in the NMERI HALOCARBON DATABASE are referenced. The citation information and keywords for literature references are provided. Online searches of literature databases were conducted for all aspects of fire suppression/combustion related to the compounds of interest.

Each field within the NMERI HALOCARBON DATABASE contains a reference number corresponding to a library document to give the sources for the information contained in the database. Users can search the literature database under reference number, author, title, subject, or keywords. Literature related to global warming, ozone depletion, climate change, fire suppression, photolysis, toxicity, safety, and availability have also been included.

C. DATABASE USE

The NMERI HALOCARBON DATABASE resides on a Harris HCX-9 mainframe, which is accessed via a telephone modem. Macros have been created to simplify database searching. When a user logs on the mainframe, the database program is called up and a login prompt is obtained (Figure A-2). The user enters an assigned login name and password to obtain access to the database information.

Database information is accessed with menus, as illustrated in Figures A-2 through A-4. In order to obtain literature information related to fire suppression/combustion or other categories, the user selects number 2 and number 11 in Figures A-3 and A-4, respectively.

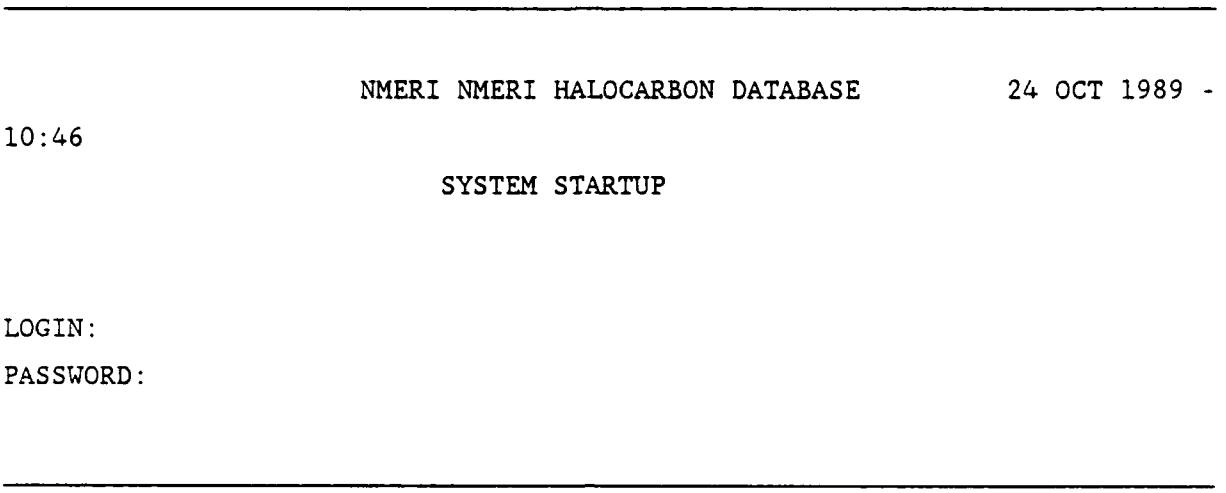


Figure A-2. NMERI HALOCARBON DATABASE Login Prompt.

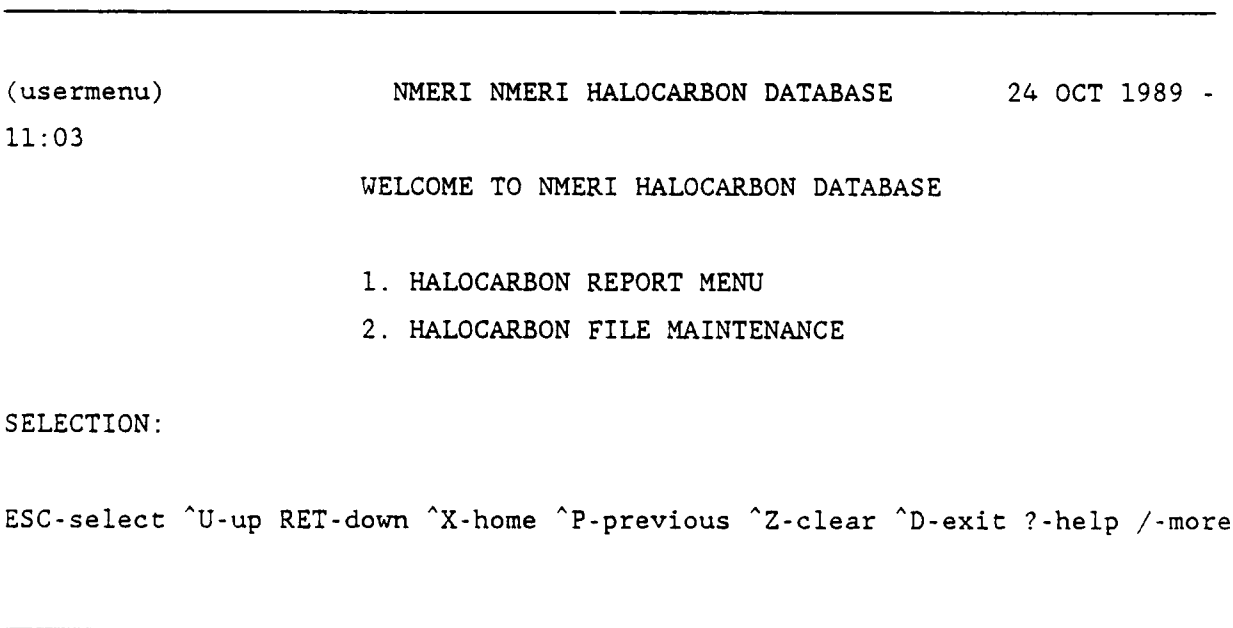


Figure A-3. Report or Maintenance Selection Menu.

(halmnt) NMERI NMERI HALOCARBON DATABASE 24 OCT 1989 - 11:07

HALOCARBON FILE MAINTENANCE

1. General Information
2. Physical/Chemical Information
3. Environmental Information
4. Laboratory Information
5. Laboratory Testing Information
6. Toxicity Information
7. Human Toxicity Information
8. Rat Toxicity Information
9. Mouse Toxicity Information
10. Rabbit Toxicity Information
11. Library Maintenance
12. Labdata Non-Halon
13. Safety Maintenance

SELECTION:

ESC-select ^U-up RET-down ^X-home ^P-previous ^Z-clear ^D-exit ?-help /-more

Figure A-4. Maintenance Selection Menu.

The fields shown in Figure A-5 are contained in the Library Maintenance portion of the NMERI HALOCARBON DATABASE. These fields contain information on references to fire suppression/combustion and several other subjects.

```
(libry)                NMERI NMERI HALOCARBON DATABASE        24 OCT 1989 -
11:12

                              Library Maintenance

Refno      : [......]
Location   : [....................]
Pending    : [.]                              Date Input: [...........]
Authors    : [.....................................................]
             [.....................................................]
             [.....................................................]
Title      : [.....................................................]
             [.....................................................]
             [.....................................................]
Journal    : [.....................................................]
Vol No     : [....................]    Issue     : [....................]

Country    : [....................]    Publisher : [....................]

Year       : [....................]    Pageno    : [....................]

Keywords   : [.....................................................]
             [.....................................................]
Subjcode   : [....................]    Refsource :  [....................]


(I)NQUIRE, (A)DD, (M)ODIFY, (D)ELETE  [.]
```

Figure A-5. Typical Literature Information Fields Contained in the NMERI HALOCARBON DATABASE.

Once at the literature maintenance screen shown in Figure A-6, the user has the option to inquire, add, modify, or delete information. Generally, users select the inquire mode by typing "i" or "I" when prompted. The user can then go to any field and type in matching criteria for the field of interest or use the character "*" as a wild card. For example, Figure A-6 shows an inquiry of all publications authored by Booth contained in the NMERI HALOCARBON DATABASE. Note the change in the user instruction at the bottom of the screen (Figure A-6). The result of the author inquiry is shown on Figure A-7. The inquiry shows that three articles authored by Booth are contained in the database. Information for the first one is shown.

```
(libry)                NMERI NMERI HALOCARBON DATABASE        24 OCT 1989 -
11:12

                              Library Maintenance

Refno      : [......]
Location   : [...................]
Pending    : [.]                              Date Input: [...........]
Authors    : [*BOOTH*.....................................................]
             [.....................................................................]
             [.....................................................................]
Title      : [.....................................................................]
             [.....................................................................]
             [.....................................................................]
Journal    : [.....................................................................]
Vol No     : [...................]    Issue     : [...................]

Country    : [...................]    Publisher : [...................]

Year       : [...................]    Pageno    : [...................]

Keywords   : [.....................................................................]
             [.....................................................................]
Subjcode   : [...................]    Refsource :  [...................]


Begin search (CTRL E), Clear field (CTRL Z), Exit (CTRL X)   <-Note change
```

Figure A-6. Example Inquiry of the Author Field of the NMERI HALOCARBON DATABASE.

(libry) NMERI NMERI HALOCARBON DATABASE 24 OCT 1989 -
11:35
(I)NQUIRE Library Maintenance

Refno : 200
Location : COMBUSTION
Pending : F Date Input: **/**/**
Authors : HIRST, R.;BOOTH, K.

Title : MEASUREMENT OF FLAME-EXTINGUISHING CONCENTRATION

Journal : FIRE TECHNOLOGY
Vol No : 13 Issue :
Country : Publisher :
Year : 1977 Pageno : 296
Keywords :

Subjcode : S Refsource :

(N)EXT, (P)REVIOUS, (S)TOP
searched: 2054 selected: 3 current: 1

Figure A-7. Result of the Inquiry Shown in Figure A-6.

A complete users' manual and the IBM PC compatible version of the NMERI HALOCARBON DATABASE will soon be available. References 5, 33, and 34 describe additional features and user instructions for the database.

REFERENCES

1. Tapscott, R. E., and Morehouse, E. T., Jr., Next-Generation Fire Extinguishing Agent, Phase I - Suppression Concepts, NMERI 3-31, Task Report (Vol. 1 of 5), Engineering and Services Laboratory, Air Force Engineering and Services Center, Tyndall AFB, FL, July 1987.

2. Tapscott, R. E., May, J. H., Moore, J. P., Lee, M. E., and Walker, J. L., Next-Generation Fire Extinguishing Agent, Phase II -- Laboratory Tests and Scoping Trials, ESL-TR-87-03, Vol. 2 of 5, Engineering and Services Laboratory, Air Force Engineering and Services Center, Tyndall AFB, FL, August 1989.

3. Tapscott, R. E., Moore, J. P., Lee, M. E., Watson, J. D., and Morehouse, E. T., Next-Generation Fire Extinguishing Agent, Phase III -- Initiation of Training Agent Development, ESL-TR-87-03, Vol. 3 of 5, Engineering and Services Laboratory, Air Force Engineering and Services Center, Tyndall AFB, FL, August 1989.

4. Tapscott, R. E., Lee, M. E., Watson, J. D., Nimitz, J. S., and Rodriguez, M. L., Next-Generation Fire Extinguishing Agent, Phase IV -- Foundation for New Training Agent Development, ESL-TR-87-03, Vol. 4 of 5, Engineering and Services Laboratory, Air Force Engineering and Services Center, Tyndall AFB, FL, June 1989.

5. Tapscott, R. E., Lee, M. E., Moore, T. A., Moore, J. P., Nimitz, J. S., Skaggs, S. R., and Floden, J. R., Next-Generation Fire Extinguishing Agent, Phase V -- Initiation of Halon Replacement Development, ESL-TR-87-03, Vol. 5 of 5, Engineering and Services Laboratory, Air Force Engineering and Services Center, Tyndall AFB, FL, March 1989.

6. Brabson, D., Tapscott, R. E., and Morehouse, E. T., Initial Fire Suppression Reactions of Halons, Phase I -- Development of Experimental Approach, NMERI WA3-67, Task Report, Engineering and Services Laboratory, Air Force Engineering and Services Center, Tyndall AFB, Florida, July 1988.

7. Creitz, E. C., "Inhibition of Diffusion Flames by Methyl Bromide and Trifluoromethyl Bromide Applied to the Fuel and Oxygen Sides of the Reaction Zone," Journal of Research of the National Bureau of Standards, Section A., Physics and Chemistry, Vol. 65, pp. 389-396, 1961.

8. Miller, J. A., and Fisk, G. A., "Combustion Chemistry," Chemical Engineering News, pp. 22-46, 31 August 1987.

9. Jenkins, F. A., and White, H. E., Fundamentals of Optics, 3rd Edition, McGraw-Hill Book Company, New York, 1957.

10. Alkemade, C. Th. J., and Herrmann, R., Fundamentals of Analytical Flame Spectroscopy, Adam Hilger Ltd., Bristol, 1979.

11. Zinman, W. G., and Bogdon, S. I., "Influence of Vibration-Rotation Interaction on the Rotational 'Temperature' Determined from an Electronic OH Transition," The Journal of Chemical Physics, Vol. 40, p. 588, 1964.

12. Dieke, G. H., and Crosswhite, H. M., "The Ultraviolet Bands of OH," Journal of Quantitative Spectroscopy and Radiative Transfer, Vol. 2, pp. 97-199, 1961.

13. Penner, S. S., Wang, C. P., and Bahadori, M. Y., "Laser Diagnostics Applied to Combustion Systems," Twentieth Symposium (International) on Combustion, The Combustion Institute, Pittsburgh, pp. 1149-1176, 1984.

14. Muller-Dethlefs, K., and Weinberg, F. J., "Burning Velocity Measurement Based on Laser Rayleigh Scattering," 17th Syposium (International) on Combustion, The Combustion Institute, Pittsburgh, pp. 985-992, 1979.

15. Lapp, M., and Penney, C. M., eds., Laser Raman Gas Diagnostics, Plenum Press, London, 1974.

16. Lapp, M., and Hartley, D. L., "Raman Scattering Studies of Combustion," Combustion Science and Technology, Vol. 13, pp. 199-210, 1976.

17. West, Michael, A., ed., Lasers in Chemistry, Elsevier Scientific Publishing Company, Amsterdam, 1977.

18. Doppelbauer, J., and Leyendecker, G., "On Temperature Determination from Rotational Raman Line Intensities," Applied Spectroscopy, Vol. 40, No. 6, p. 831, 1986.

19. Wilson, E. B., Jr., Decius, J. C., and Cross, P. C., Molecular Vibrations, McGraw-Hill Book Company, New York, 1955.

20. Eggers, D. F., Jr., Gregory, N. W., Halsey, G. D., Jr., and Rabinovitch, B. S., Physical Chemistry, pp. 424-487, John Wiley and Sons, New York, 1964.

21. Jennings, D. E., Weber, A., and Brault, J. W., "Raman Spectroscopy of Gases with a Fourier Transform Spectrometer," Applied Optics, Vol. 25, p. 284, 1986.

22. Jones, D. G., and Mackie, J. C., "Evaluation of C2 Resonance Fluorescence as a Technique for Transient Flame Studies," Combustion and Flame, Vol. 27, pp. 143-146, 1976.

23. Weast, R. C., ed., CRC Handbook of Chemistry and Physics, 69th edition, CRC Press, Inc., Boca Raton, 1988-1989.

24. Dasch, C. J., and Bechtel, J. H., "Spontaneous Raman Scattering by Ground-State Oxygen Atoms," Optics Letters, Vol. 6, p. 36, 1981.

25. Chang, H., and Chen, S., "Photodissociation of Bromine and the Electronic Raman Spectra of Br Under Argon Ion Laser Light," Journal of Spectroscopy, Vol. 17, pp. 453-458, 1986.

26. Westbrook, C. K., "Numerical Modeling of Flame Inhibition by Halon 1301," Combustion Science and Technology, Vol. 34, pp. 201-225, 1983.

27. Larsen, E. R., "Halogenated Fire Extinguishants: Flame Suppression by a Physical Mechanism?," Halogenated Fire Suppressants, R. G. Gann, ed., ACS Symposium Series 16, American Chemical Society, Washington, DC, pp. 376-402, 1975.

28. Wuebbles, D. J., The Relative Efficiency of a Number of Halocarbons for Destroying Stratospheric Ozone, UCID 18924, Lawrence Livermore National Laboratory, January 1981.

29. Gontkovskaya, K. A., and Gontkovskaya, V. T., "Kinetics of Hydrogen Oxidation," Combustion Science and Technology, Vol. 17, p. 143, 1977.

30. Westbrook, C. K., "Inhibition of Hydrocarbon Oxidation in Laminar Flames and Detonations by Halogenated Compounds," 19th Symposium (International) on Combustion, The Combustion Institute, Pittsburgh, pp. 127-141, 1982.

31. The Harris HCX-9 main frame operates under UNIX System V with 8 Mbytes of RAM, 600 Mbytes of disk storage, 9-track tape drive, and associated printers. It has a 100 nanosecond clock and operates at 7.5 MIPS. It is currently configured with 48 user ports and 4 remote access ports. For more information, contact HARRIS Corporation, Computer Systems Division, 16001 Dallas Parkway, Dallas, Texas 75248-2155; telephone (214) 386-2155.

32. UNIFY is an ANSI-standard SQL based Relational Database Management System designed to optimize run-time performance in transaction oriented environments. The PC version uses an SOS/Unix bridge that allows compatibility between PC and mainframe applications. For more information, contact UNIFY Corporation, 4000 Kruse Way Place, Building 3, Suite 200, Lake Oswego, Oregon 97035; telephone (800)-24-UNIFY.

33. Moore, T. A., Moore, J. P., Rodriguez, M. L., and Tapscott, R. E., NMERI HALOCARBON DATABASE, NMERI OC90/7, Air Force Engineering and Services Center, Tyndall Air Force Base, FL, Preliminary Report, June 1989.

34. Tapscott, R. E., Moore, T. A., and Moore, J. P., A Database of Halocarbon Candidates for Halon and CFC Alternatives, paper presented at International Conference on CFC and Halon Alternatives, Washington, DC, 10-11 October 1989.

(The reverse of this page is blank.)